The Role of Passive Film Growth Kinetics and Properties in Stress Corrosion and Crevice Corrosion Susceptibility

J. Kruger and J. R. Ambrose

Corrosion and Electrodeposition Section
Metallurgy Division
Institute for Materials Research
National Bureau of Standards

THE ROLE OF PASSIVE FILM GROWTH KINETICS AND PROPERTIES IN STRESS CORROSION AND CREVICE CORROSION SUSCEPTIBILITY

J. Kruger and J. R. Ambrose

Corrosion and Electrodeposition Section
Metallurgy Division
Institute for Materials Research
National Bureau of Standards

July 1973

Technical Summary Report Number 4

U. S. DEPARTMENT OF COMMERCE, Frederick B. Dent, Secretary

NATIONAL BUREAU OF STANDARDS, Richard W. Roberts, Director

REPASSIVATION KINETICS OF 304 STAINLESS STEEL
IN CHLORIDE SOLUTIONS AT ROOM TEMPERATURE

J. R. Ambrose and J. Kruger
Institute for Materials Research
National Bureau of Standards
Washington, D. C.

ABSTRACT

Repassivation kinetics of an AISI 304 stainless steel have been determined
in 1.0N NaCl solutions using the triboellipsometry technique which permits
measurement of film growth and total reaction rates following removal of the
surface film by abrasion. Although deoxygenation of the solution resulted in
little change in either film growth kinetics or the ratio of total change to
film thickness (R_p), changing the solution pH affected both the mechanism and
rate of film growth which resulted in increased rates of metal dissolution in
acidic (pH3) and basic (pH11) solutions.

In neutral 1.0N NaCl solutions, where film growth increased with more
positive applied potentials, the rate of metal dissolution during the
repassivation transient was initially highest at the corrosion potential, but
decreased with time as the surface became passivated.

REPASSIVATION KINETICS OF 304 STAINLESS STEEL
IN CHLORIDE SOLUTIONS AT ROOM TEMPERATURE

J. R. Ambrose and J. Kruger
Institute for Materials Research
National Bureau of Standards
Washington, D.C.

A number of workers[1-5] in recent years, most notably Scully[1]
and Staehle,[2] have pointed out the important role that repassivation
kinetics plays in the complex processes governing stress corrosion cracking
(SCC). Scully was among the first to emphasize that the process of re-
passivation that occurs when protective films on metal surfaces are
broken by slip step emergence upon stressing the metal is probably the
step in the chain of events leading to cracking that is most sensitive
to environmental factors (pH, potential, oxygen concentration, anion and
cation nature and concentrations, and others). Moreover, because most
mechanisms of SCC require that an unprotected surface be available for
either dissolution, hydrogen entry, or adsorption of bond breaking species
to take place, the rate at which that surface becomes reprotected can
be crucial.

Attempts to measure the repassivation kinetics of austenitic
stainless steels have been made by Hoar and Hines,[3] Shibata and Staehle,[4]
and Lees and Hoar.[5] All of these studies used the straining electrode
or scratching techniques, measuring current transients. A problem with
these techniques is that one cannot separate out the current involved
in dissolution and other processes from that involved in film formation
leading to repassivation. Since the crucial process to study is the
effectiveness of the repassivation on inhibiting dissolution or other

processes such as hydrogen entry, we have been developing a technique that can measure the film regrowth process alone and separate it from the total current involved in repassivation. This technique called tribo-ellipsometry is described elsewhere.[6] In addition to measuring the rate of film regrowth it is able to measure for a repassivation transient the repassivation ratio, R_p, which is defined as follows: $R_p = \frac{Q_T}{x} = \frac{1}{k}(1 + \frac{Q_d}{Q_x})$, where Q_t is the total charge consumed in the repassivation process, x is the thickness of the film, Q_d is the charge involved in dissolution and other non-film forming processes, and Q_x is the charge involved in film formation. The k is a constant that converts x, the film thickness, to charge. R_p is thus a measure of the effectiveness of the repassivation process.

In this study the first attempts to study the repassivation kinetics of 304 stainless steel in chloride solutions at room temperature by tribo-ellipsometry are described. Besides its practical importance, this alloy cracks transgranularly, thereby offering an ideal system to study tribo-ellipsometrically, since film thickness data are obtained for that surface where crack initiation occurs. These studies provide direct measurements of the rate of repassivation that Scully[1] pointed out were needed to assess environmental factors in SCC. Because such factors as pH, oxygen concentration, and potential are altered in the environment of a growing crack, their effect on repassivation was studied. Finally, because tribo-ellipsometry is able to measure the time of repassivation t_p and distance of crack advance, L, during this time (assuming crack advance is due to dissolution) our measurements are compared to predictions of a new film rupture theory by Vermilyea[17] which calculates L from

assumed stress and strain conditions.

EXPERIMENTAL

Measurement Technique

The tribo-ellipsometric studies were carried out using the techniques described in earlier work.[6,7] However, certain modification of the technique was required for the 304 stainless steel/sodium chloride solution system since, under the solution agitation conditions produced by the abrasion device, film thicknesses and growth rates were of a magnitude to be beyond the sensitivity of the ellipsometric detection apparatus ($x < 0.1$ nm; $dx/dt \simeq 0$, $t_p < 10$ msec). This would not be unusual for a system in which film growth kinetics are determined by mass transport in the solution. Therefore, surface films were removed by abrasion at potentials where film regrowth would not be expected to occur (i.e., -1000 mV SHE). Following measurement of ellipsometric optical parameters, the potential was stepped to those values of interest in this study using a fast rise two-channel potentiostat. Since cessation of the cathodic hydrogen evolution which occurs at those starting potentials would result in an ellipsometric light intensity increase upon potential step, modification of the off-null ellipsometry procedure[8] was employed such that film growth would give light intensity decreases. Growth and current transients were displayed on an oscilloscope and the recordings analyzed as in previous studies.[6,7]

Materials

The material used in this study was a commercially available AISI 304 stainless steel fabricated into cylindrical specimens 1.905 cm in

diameter and 0.635 cm thick. Specimens were mechanically polished through successive grits of silicon carbide metallographic papers and followed by rotary polishing on nylon cloth with 6 micron diamond paste.

The principal solution used was a 1.0N NaCl solution prepared from ACS reagent grade chemical and distilled water (7.0×10^{-7} ohm^{-1} cm^{-1}). pH adjustment was made with aliquots of 1.0N NaOH or HCl solution. Solution deoxygenation was accomplished by dispersing helium gas (99%) through the solution.

RESULTS

Because one of the important variables in the crack environment is the pH of the solution, the major emphasis was placed on studying the effect of pH on repassivation kinetics. A few experiments examined the effect of lowering the oxygen concentration and changing the potential to values other than that measured at open circuit which could also change in the crack environment.

A compilation of the repassivation transient data measured under all of the conditions studied is given in Table 1. The distance of each advance, L, during the time of repassivation, t_p, which is listed in the table was calculated on the following basis: the linear log-log plot of current vs time was extrapolated to a time of 1 msec.

This particular time was selected in order to avoid complications arising from double layer charging effects on the rather large surface area of the specimen used (2.85 cm^2). The value of current at this time, designated i_{max}, was assumed to flow uniformly to all areas of exposed metal not yet covered by the passivating film. At t_p, then, one would

5

expect maximum penetration by metal dissolution at these areas of bare metal last to be protected, and that this distance of penetration would correspond approximately to the distance of crack advance, L.

L was then calculated from

$$L = \frac{i_{max}M}{zFA\rho} \, tm \qquad [1]$$

where M is the average molecular weight of the film formed, assuming it to be 18% Cr_2O_3, 8% NiO, and 78% Fe_2O_3; A is the area of the surface exposed by abrasion; ρ is the average density of the oxides used to calculate M, F the Faraday and z the valance of the moving species and is assumed to be +2.

Effect of pH

These experiments were carried out at room temperature at pH 3, 7, and 11. The reasons for the choice of these values were as follows: a) The pH 3 solution is at the approximate value[9] found near crack tips for a large number of different steels; b) The pH 7 solution is the neutral value that exists in many natural environments and is important in crack initiation processes; c) The pH 11 solution attempts to simulate conditions that a recent theoretical study[10] indicates may exist right at the crack tip surface. This study suggests that the metal ions produced by dissolution may have time to diffuse away from the surface if the hydrolysis reaction which produces hydrogen ions is sluggish. Thus, the pH is lowered away from the surface while at the surface the discharge of diffusion limited hydrogen ions raises the pH.

Fig. 1 shows the film growth kinetics for the three pH solutions at a potential of +90 mV (SHE), the open circuit potential for the pH 7

6

solution. For cracking in a conductive neutral environment this would probably be the controlling potential. It can be seen that the rate of repassivation is greatest for the neutral solution and least for the acidic. Moreover, because the plot of film thickness vs log time is linear for the films grown in the pH 7 and 11 solutions, the rate law governing the film growth process is directly logarithmic. This suggests that the film forms by a field assisted growth mechanism[11] and, if this is so, that the film is probably non-porous. The film growth law in the pH 3 solution appears to follow a more complex mechanism. It is, as would be expected, thinner than those formed in the pH 7 or 11 solutions for a given time of growth. Therefore, based on the film growth rate data, the repassivation rate, $\frac{dx}{dt}$, would have the following order with respect to pH:

$$\left(\frac{dx}{dt}\right)_{pH_3} < \left(\frac{dx}{dt}\right)_{pH_{11}} < \left(\frac{dx}{dt}\right)_{pH_7}$$

In addition to film growth kinetics, the tribo-ellipsometric technique also permits determination of the kinetics of current decay. Fig. 2 is a log-log plot of current vs time for the 3 different pH solutions studied. The rate of current decay is essentially the same for the pH 7 and 11 solutions but is lower for the pH 3. Moreover, while the magnitude of the anodic current appears lower for the pH 3 at the beginning of the passivation process, it eventually exceeds the values found for the other two solutions. It is quite likely that the anodic current measured for the pH 3 solution probably is in error due to a cathodic component from the hydrogen reduction reaction in the more acidic solution. Thus, the values measured for the pH 3 solution are undoubtedly low.

When we now combine the current measurements with those of film
formation we can determine the repassivation ratio, R_p, a measure of the
effectiveness of repassivation. Fig. 3 shows the variation of R_p with
time. The order is the reverse of that for film growth rate,

$$R_p(pH_7) < R_p(pH_{11}) < R_p(pH_3)$$

Also, becuase as just pointed out, the current values for pH 3 are
probably low, the R_p values for that solution must be even higher than
those shown on Fig. 3.

Effect of Oxygen Concentration

A few experiments comparing the repassivation rates of 304 stainless
steel in air saturated and deaerated pH 7 1N NaCl solution were carried
out.

As Figs. 4, 5, and 6 show, lowering the oxygen concentration does
not affect the rate of film growth, current decay, or R_p. However,
the magnitude of these parameters were in all cases slightly lowered.
Thus, there was no mechanistic change, only a slight lowering in the
amount of film formed and the amount of current involved in the most
prevalent anodic processes (film growth and metal dissolution). Except
for the effect of oxygen on the open circuit potential which was purposely
circumvented in these experiments, the effect of oxygen on repassivation
kinetics appears to be minimal. The effect of potential and oxygen con-
centration will be examined in the next section.

Effect of Potential

Potential of the repassivating surface plays an important role
in determining stress corrosion susceptibility.[12] These experiments

therefore inviestigate the effect of potential on repassivation kinetics. Because the potential value at the tip of a crack is probably less than that measured at the surface of a specimen, we have looked at more negative potentials than the open circuit value measured for an air saturated 1N NaCl solution [+90 mV (SHE)].

The film formation kinetics in a pH 7 deoxygenated solution at +90, -134, and -263 mv SHE are shown in Fig. 7. The -134 value is the open circuit potential for a deoxygenated pH 7 solution, and -263 mV is the value for the same solution after a number of abrasion cycles, a condition that produces a high concentration of reduction products and metal ions that may simulate more closely the conditions after crack propagation has progressed. It can be seen from Fig. 7 that at -134 mV the mechanism of formation is initially the same as at the higher potential but that it changes at around 40 msec and growth virtually stops. This is even more pronounced at -263 mV. The current decay behavior (Fig. 8) is somewhat similar to the higher potentials while the variation in R_p (Fig. 9) is quite irregular.

DISCUSSION

It is evident from the repassivation data in Table 1 that the repassivation process is least effective for surfaces exposed to the pH 3 solutions. Besides the fact that the time of repassivation and R_p are 2-3 times as large as they are for the pH 7 and 11 solutions, the ultimate films formed are thinner. Moreover, because the currents measured during repassivation in the pH 3 solution are probably not the true values since there exists in the acidic solution a considerable cathodic component, the effectiveness of repassivation, R_p is even less than Table 1 would

indicate. These results therefore indicate, not surprisingly, that the lowering of pH in an advancing crack does inhibit repassivation in chloride environments. These results do not, however, settle the question of whether the mechanism of SCC for austenitic stainless steel is a slip-dissolution one or one involving the entry of hydrogen into the lattice which promotes the formation of martensite or some other brittle phase as proposed, for example, by Troiano[13] and others.[14] They do, however, indicate that regardless of whether the mode of crack growth is due to metal dissolution or embrittlement, the conditions are present for promoting poor repassivation rates.

Susceptible conditions are also present for the pH 11 solution where the repassivation kinetics are slower than for the pH 7 solutions. There are instances of failure of austenitic steel in alkaline environments[15] albeit at higher concentrations and temperatures. As mentioned earlier, recent theoretical studies[10] indicate that if the hydrolysis reaction is slow, the pH at the immediate surface may not be too dissimilar for a pH 3 and pH 11 solution. For example, on the basis of a simple Fick's law diffusion calculation we find that the pH at the surface can be as high as 10 for a pH 3 solution, assuming a diffusion limited hydrogen reduction current of 3×10^{-4} amp/cm^2. This could be the situation within the confines of a crack where mass transport processes are rate limiting. These considerations do not explain the order of the repassivation kinetics observed for the solutions studied. They simply point out that evaluation of environmental conditions at the surface where repassivation takes place in the confinement of a crack is not straightforward. Thus, it may be that the repassivation parameters measured at pH 11 in our

experimental set-up which does not have the confining conditions of a crack may be more indicative of susceptibility. The repassivation rates for pH 3 may be too low to promote cracking and instead would result in tip blunting.

Lowering the oxygen content of the pH 7 solution does not appear to affect appreciably the repassivation process. Such a decrease in oxygen concentration would be reasonable in a propagating crack. Apparently, the main role that oxygen concentration plays is its effect on the potential. As the potential experiments indicate, the lowering of potential towards the active region does indeed affect repassivation by altering the rate and mechanism of film growth. This would agree with the ideas of Staehle[2] who pointed out that regions of susceptibility are located at potentials on the borderline between the active and passive regions and the passive and pitting, (he labels it transpassive) regions. We have not yet made studies at potentials near the pitting region because of surface roughening problems, but we hope to be able to make an approximate measure of t_p and R_p for those potentials in future experiments.

None of the measurements of repassivation rates are capable of predicting susceptibility without also knowing something about the rate of bare metal production during stressing. As a first estimate, however, it is useful to use a new theory by Vermilyea[16] who has developed a film rupture model for stress corrosion crack propagation. This theory relates the creep transient in the metal at the crack tip following film rupture and the critical strain required to rupture the protective film to the crack propagation rate as determined by the kinetics of repassivation and corrosion. Two parameters needed by the theory are L and t_p.

Using the values listed in Table 1 to calculate L by Eq [1] we can compare

our measurements to values predicted by Vermilyea's theory. The value

he calculates for the minimum value of L, L_{min}, which will allow SCC that

comes closest to our values calculated from the tribo-ellipsometric values

are based on his equation derived for a plane strain condition with a

strain gradient of 1/r where r is the distance in the plane of the crack

from the center of curvature of the crack tip. This equation is

$$L_{min} = \frac{2\epsilon_\rho \epsilon_c X_0}{2(\epsilon_\rho - 2\epsilon_c)} \qquad [2]$$

where ϵ_p is the plastic strain at the crack tip, ϵ_c is the critical

strain for film rupture, and X_0 = distance between ductile rupture void

centers. Assuming $\epsilon_p \gg 2\epsilon_c$ and $X_0 = 5.08 \times 10 cm^{-4}$, we get a value for

L_{min} of 7.62 x 10^{-7} cm. Since the values listed in Table 1 are all of

the order of magnitude or somewhat greater, on the basis of repassivation

kinetics only, we would predict that under conditions of plane strain

with a strain gradient of 1/r 304 stainless steel would be susceptible

to SCC. Obviously, both Vermilyea's theory and our calculations of L

have a number of assumptions and simplifications so that, in practice,

this prediction is suspect. Also in practice austenitic stainless steel

in chloride solutions of our concentrations at room temperature are not

very susceptible to SCC. What is needed is more and better measurements

of the mechanical and chemical parameters. The constant strain technique

described by Parkins[17] offers some hope for gaining some insight into

the mechanical aspects that are most applicable to tribo-ellipsometric

measurements of repassivation kinetics. This will be the next direction

our work will take.

ACKNOWLEDGEMENT

References

1. J. C. Scully, Corr. Sci. 8, 513 (1968).

2. R. W. Staehle, "The Theory of Stress Corrosion Cracking in Alloys,"
    J. C. Scully, ed., N.A.T.O. Sci. Affairs Div., Brussels (1971) p.223.

3. T. P. Hoar and S. G. Hines, J. Iron Steel Inst. 184, 166 (1956).

4. T. Shibata and R. W. Staehle, Proc. Fifth Int. Cong. on Metallic Corr.,
    Tokyo, 1972.

5. D. J. Lees and I. P. Hoar, In preparation, reported in Proc. Int. Conf. on
    Stress Corr. Cracking and Hydrogen Embrittlement of Iron Base Alloys,
    Firminy France 1973, to be published by N.A.C.E., Houston.

6. J. R. Ambrose and J. Kruger, Corrosion 28, 30 (1972).

7. J. R. Ambrose and J. Kruger, Proc. Fifth Int. Cong. on Met. Corr., Tokyo (1972).

8. J. J. Carroll and A. J. Melmed, Surf. Sci. 16, 251 (1969).

9. G. Sandoz, C. T. Fujii and B. F. Brown, Con. Sci. 10, 839 (1970).

10. J. R. Ambrose, U. Bectocci and S. R. Coriell, In preparation.

11. L. Young, "Anodic Oxide Films," Academic Press, New York (1961) p.14.

12. H. H. Uhlig and F. Cook, Jr., J. Electrochem. Soc. 116, 173 (1969).

13. A. R. Troiano, Trans. A.S.M. 52, 54 (1960).

14. See page 233 of Ref. (2).

15. D. V. Subrahmanayam and R. W. Staehle, See page 228, Ref. (2).

16. D. A. Vermilyea, "A Film Rupture Model for Stress Corrosion Crack Propagation,"
    General Electric Co. Corporate Research and Development Report No. 73CRD063,
    Feb. 1973.

Table 1

pH	O_2	mV(SHE) Potential	msec t_p	R_p	R_p^*	L, cm
3	yes	+090	120	5.96	5.66	1.26×10^{-6}
7	yes	+090	65	1.69	1.60	2.30×10^{-6}
11	yes	+090	35	3.33	3.16	1.10×10^{-6}
7	no	-134	70	1.45	1.53	1.47×10^{-6}
7	no	-263	60	1.25	1.35	9.50×10^{-7}
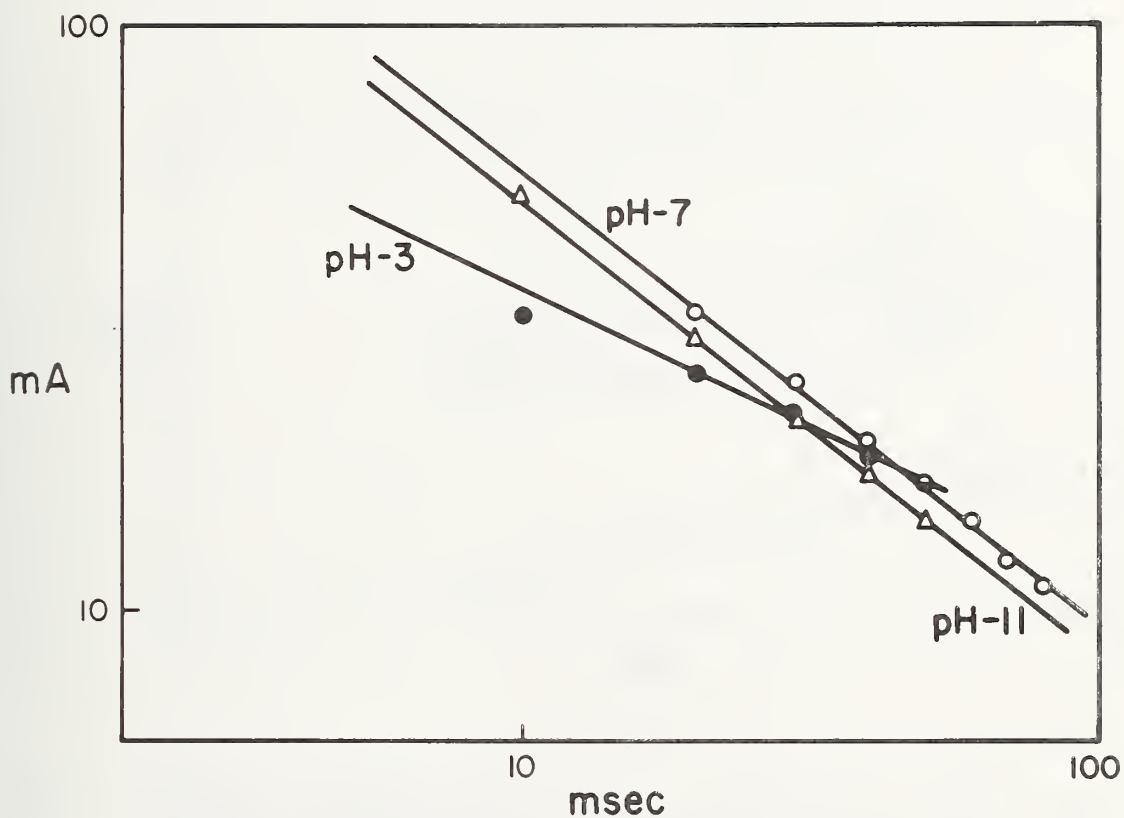
Figure 2   Anodic current decay rates ($\log_{10}$ mA vs $\log_{10}$ msec) for 304
            stainless steel in air saturated 1.0N NaCl (pH 3, 7 and 11)
            at +90 mV (SHE) following removal of surface film by abrasion
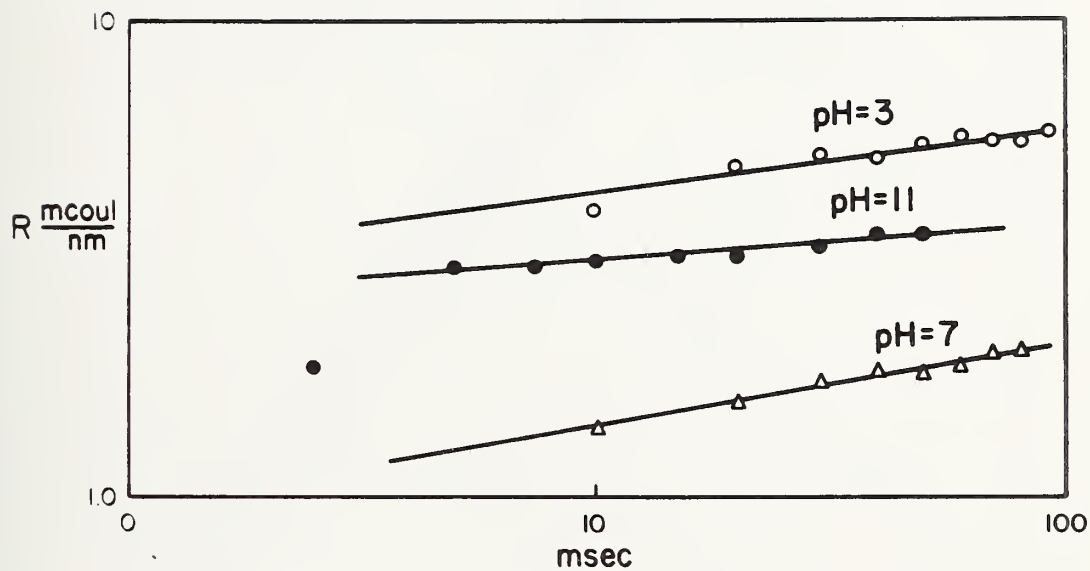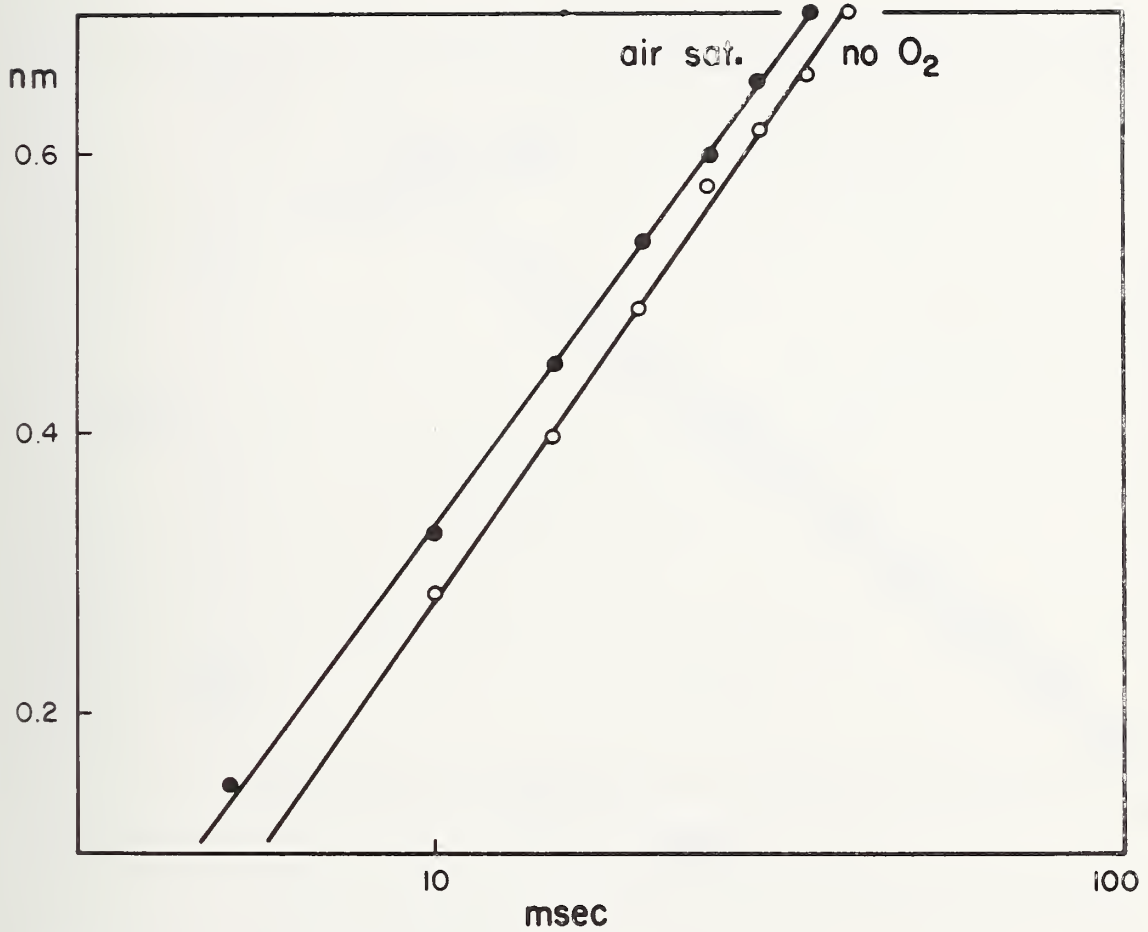   at -1000 mV (SHE).

Figure 3   Changes in Repassivation Ratio, R_p ($\log_{10} R_p$ vs $\log_{10}$ msec) for
304 stainless steel in air saturated 1.0N NaCl (pH 3, 7 and 11)
at +90 mV (SHE) following removal of surface film by abrasion at
-1000 mV (SHE).

18

Figure 4   Film growth rates (nm vs $\log_{10}$ msec) for 304 stainless steel in air saturated and deaerated 1.0N NaCl solution (pH 7) at ÷90 mV (SHE) following removal of surface film by abrasion at -1000 mV (SHE).
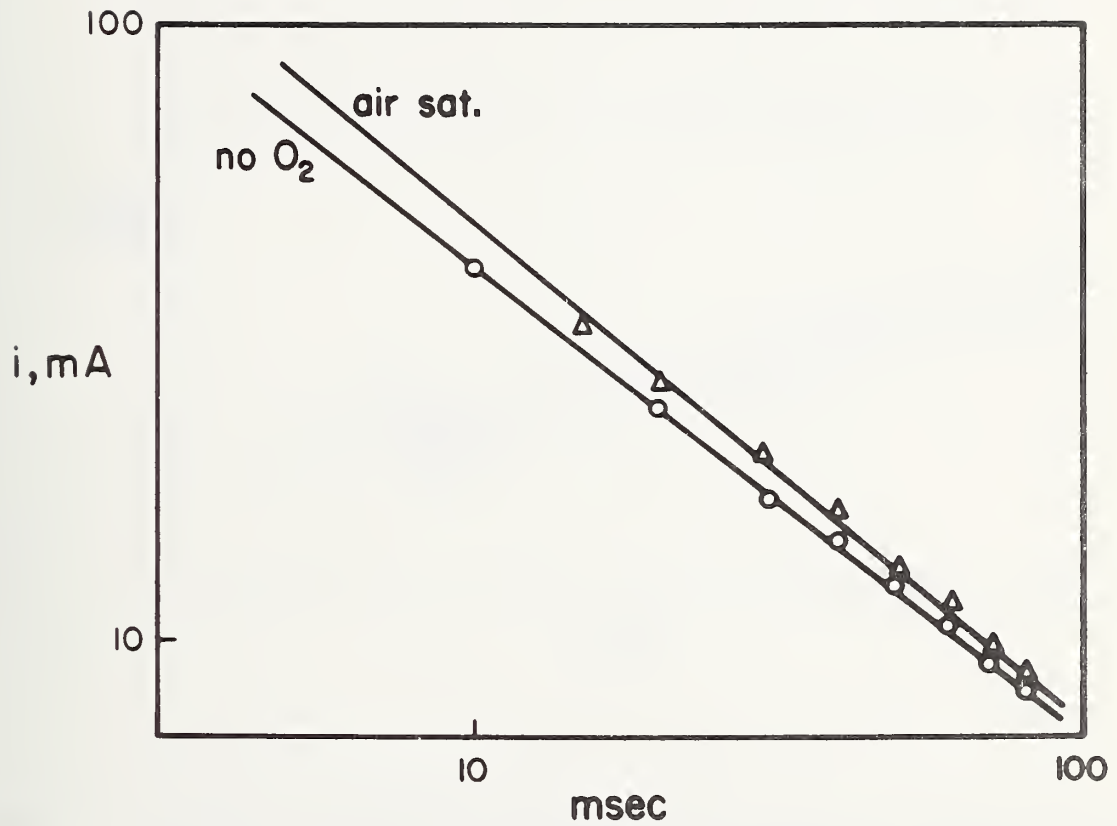
19

Figure 5   Anodic current decay rates ($\log_{10}$ mA vs. $\log_{10}$ msec) for 304
stainless steel in air saturated and deaerated 1.0N NaCl solution
(pH7) at +90 mV (SHE) following removal of surface film by abrasion
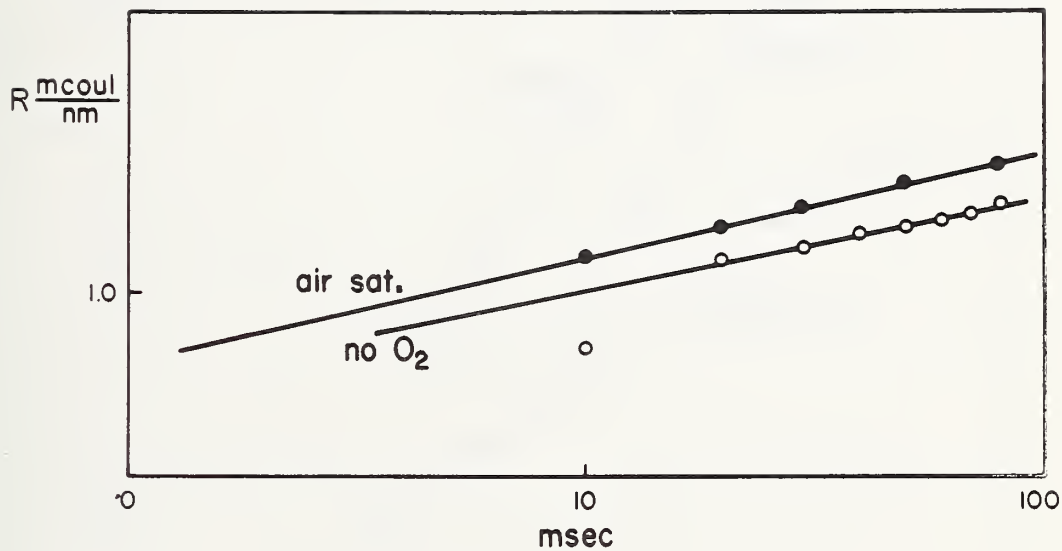at -1000 mV (SHE).

Figure 6   Changes in Repassivation Ratio R_p ($\log_{10} R_p$ vs $\log_{10}$ msec) for 304 stainless steel in air saturated and deaerated 1.0N NaCl solution (pH7) at 90 mV (SHE) following removal of surface film by abrasion at -1000 mV (SHE).
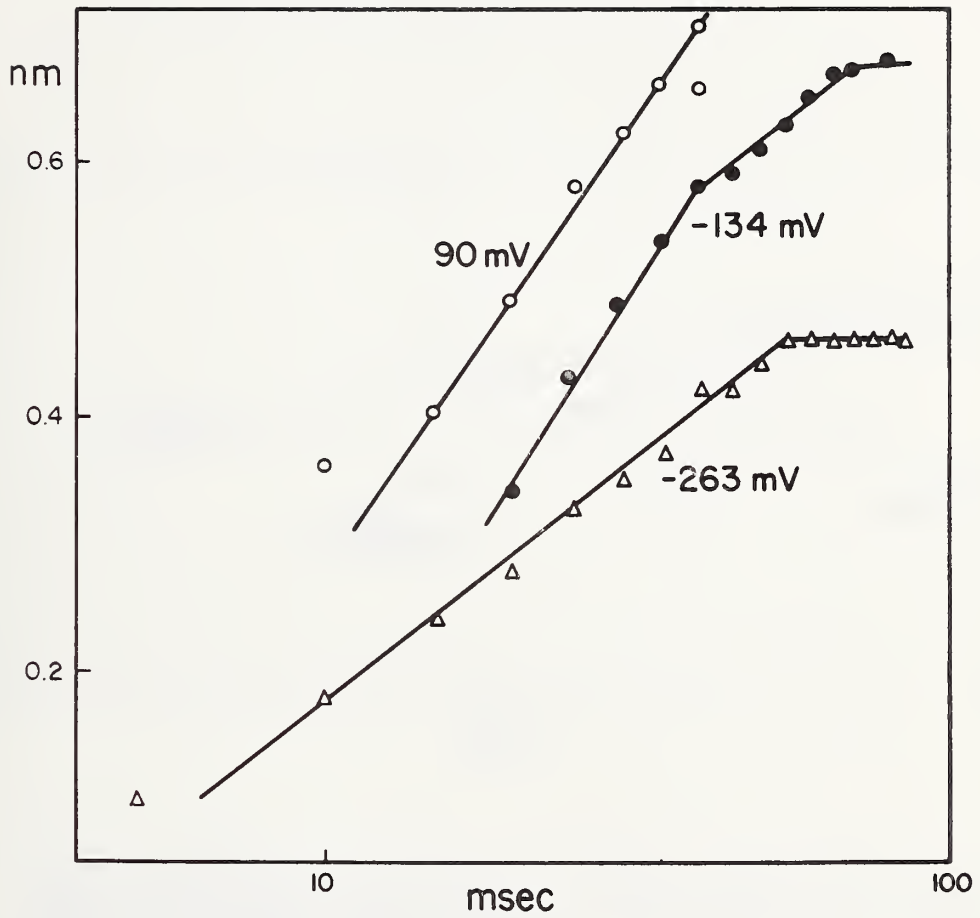
Figure 7   Effect of applied potential (+90, -134 and -263 mV SHE) on film
            growth rates (nm vs $\log_{10}$ msec) for 304 stainless steel in air
            saturated 1.0N NaCl (pH7) following removal of surface film by
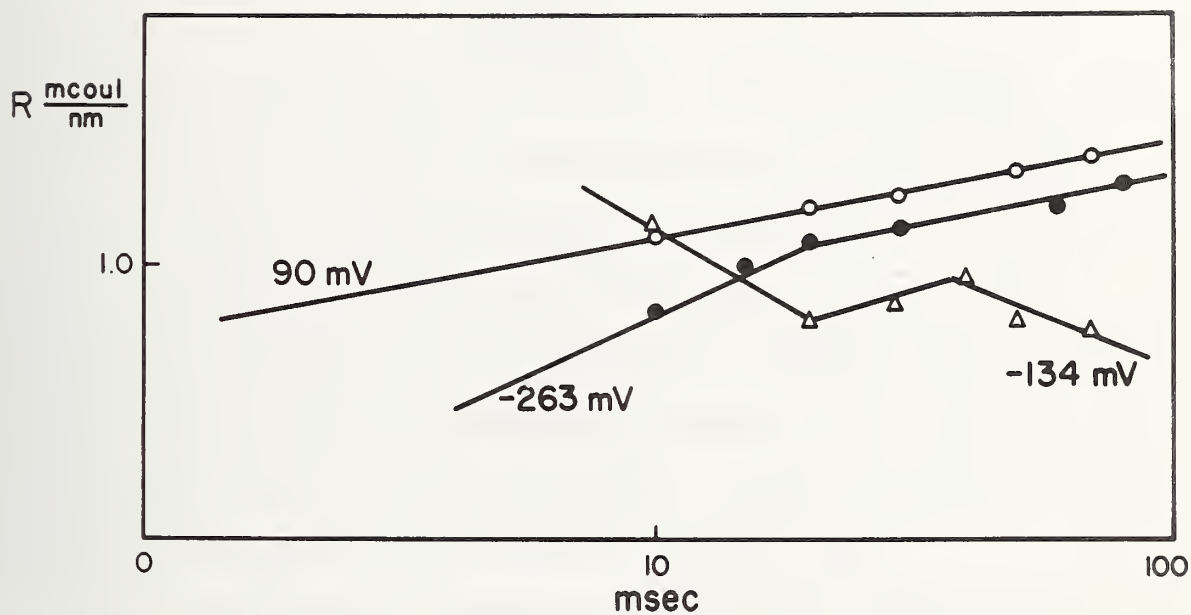   abrasion at -1000 mV (SHE).

Figure 8   Effect of applied potential (+90, -134 and -263 mV SHE) on the
Repassivation Ratio, R_p ($\log_{10} R_p$ vs $\log_{10}$ msec) for 304 stainless
steel in 1.0N NaCl (pH7) following removal of surface film by
abrasion at -1000 mV (SHE).

Part II. To be presented at National Meeting,
Electrochemical Society, Boston, Massachusetts, October 1973

A New Technique for Studying Crevice Corrosion by Ellipsometry

J. R. Ambrose and J. Kruger
National Bureau of Standards
Institute for Materials Research
Washington, D.C.

ABSTRACT

The early stages of crevice corrosion of AISI 304 stainless steel in 1.0N NaCl solution have been detected using the ellipsometer to measure changes in optical properties occurring within the crevice between a polished metal surface and a glass plate. Changes in the ellipsometric parameters Δ and ψ begin almost immediately upon creation of the crevice and can be interpreted as resulting from a build-up of soluble species within the crevice solution, followed by an overall thinning of the protective film and general corrosion attack.

Such optical changes could not be reproduced by deoxygenation of the bulk solution without the presence of a crevice nor were they observed during experiments using a Ti-8Al-1Mo-1V alloy, which is not susceptible to crevice corrosion in the 1.0N NaCl at room temperature.

A New Technique for Studying Crevice Corrosion by Ellipsometry

J. R. Ambrose and J. Kruger
National Bureau of Standards
Institute of Materials Research
Washington, D.C.

There has been an increasing interest in the problem of crevice
corrosion in recent years because it is now recognized that it is diffi-
cult to design systems that avoid crevices. Thus, crevice corrosion can
be the cause of many equipment failures due to corrosion.[1] Coburn[2]
has also pointed out that concentration cell crevice corrosion is the
most important example, costing industry more than any other type of
corrosion. Mechanisms based almost exclusively on electrochemical tech-
niques have been proposed which combine a version of the differential
oxygen concentration cell modified to reflect the separation of active-
passive cells by restricted mass transport.[3] Recent reviews on the
subject have discussed experimental techniques and proposed mechanisms
to account for the results obtained from such techniques,[4,5] and have
pointed out the problems arising in interpreting electrochemical data.

In order to complement the available electrochemical techniques,
a method has been devised using a glass plate to create the crevice,
which permits optical detection of changes occurring during the corrosion
process by means of ellipsometry. Use of such transparent windows for
visual observation of crevice is not new,[6,7] but the results from such
studies have been limited to detection of crevice corrosion in its ad-
vanced stages. The optical technique of ellipsometry, however, not only
permits measurement of small changes in thickness and optical properties
of surface films on metal substrates,[8] but can perhaps be used to detect

25

changes in composition of aqueous media as well. By use of this technique
it is hoped that it will be possible to interpret the electrochemical
results obtained in previous studies by being able to detect small changes
occurring in the early stages of the chain of events leading to crevice
corrosion. Since this technique mainly focuses on what happens to the
protective film on the metal in the crevice, it may be useful in develop-
ing ways to prevent film breakdown leading to crevice attack.

To investigate the practicality of such a technique in measuring
optical changes which occur during the early stages of crevice corrosion,
we have examined by means of this technique the effect of a crevice on
the behavior of   AISI 304 stainless steel in a 1.0N NaCl solution, an
environment in which this material is known to be susceptible to crevice
corrosion attack.[4] We have also compared the behavior observed for the
susceptible stainless steel to that of a titanium alloy which is not·
susceptible to crevice attack in chloride at room temperature.[4] Since
solution deoxygenation is thought to be a prime factor in establishing
the specific location for initiation of crevice corrosion, a complementary
study into the effect of solution deaeration on system electrochemistry
and protective film properties was also carried out.

EXPERIMENTAL

Apparatus

The device used to simulate a crevice in these studies is shown
in Fig. 1 and consists of a Teflon adapter which serves to position a
circular pyrex glass plate (3.175 cm diameter x 6.35 cm thick) against
the surface of a polished metal specimen. The thickness of the pyrex

disc was such that interference between the beams reflected from the metal surface and those reflected from the top of the plate did not occur (Fig. 2). The sides of the Teflon adapter were cut away in order to allow access of a bulk solution to the crevice. The lateral surfaces of the specimen were isolated from the environment by a tightly wound layer of Teflon tape in order to prevent crevice attack where it could not be observed optically. The rear surface of the specimen was similarly protected during those experiments where potentiostatic control was applied. The ellipsometer and cells were similar to those described elsewhere.[9]

Materials

The 0.635 cm thick cylindrical specimens used in this study were machined from 3/4-inch diameter AISI 304 stainless steel rod stock and Ti-8Al-1Mo-1V alloy, then drilled and tapped for mounting in an electrode assembly. The specimens were hand polished using a series of silicon carbide metallographic papers followed by rotary polishing on nylon cloth with 6 and 1 micron diamond paste. Specimens were rinsed with alcohol and dried in a hot air stream. Solutions were prepared using ACS reagent grade sodium chloride and distilled water (7.0×10^{-7} ohm^{-1} cm^{-1}). Deaeration was accomplished by dispersing 99% purity helium gas through the solution.

Experimental Procedure

Following electrode assembly and specimen polishing, the entire electrode unit was rinsed with alcohol and dried under hot air. Those specimen surfaces which were to be protected were wrapped in Teflon tape, and the electrode assembly inserted into the electrochemical cell. The

cell was flushed once, then filled with 1.0N NaCl and electrical connec-
tions made. Cell and specimen positions were adjusted in order to achieve
proper alignment for the ellipsometric measurements. Initial readings
of Δ and ψ were made within two minutes after exposure of the specimen
to the 1.0N NaCl solution. Following measurement of the open circuit
co-rosion potential, the crevice device was attached to the specimen;
the cell was repositioned for maximum optical sensitivity. Δ and ψ
were again measured within two minutes after creation of the crevice.
Δ, ψ, and current (or potential, depending on whether potentiostatic or
open circuit mode of control was used) were monitored for periods up to
approximately 2000 minutes or until crevice attack was evident. The
crevice device was then removed, and final Δ and ψ values were recorded.

RESULTS AND DISCUSSION

Effect of Solution Deoxygenation

There appears to be general agreement with the fact that oxygen
depletion within the crevice constitutes the initial phase of crevice
corrosion attack.[5] Therefore, we sought by making ellipsometric
measurements, to determine the effect of oxygen depletion on the protec-
tive film on the metal in the absence of a crevice. These measurements
give values of Δ, the relative phase retardation, and ψ, the tangent of
which is the relative amplitude reduction. For a metal with absorbing
films such as stainless steel, Δ is the parameter most sensitive to
changes in film thickness.[10] Both parameters are affected by film
optical property changes. Results for 304 stainless steel exposed to
1.0N NaCl without a crevice, in both potentiostatic and open circuit modes,

are shown in Figs. 3 and 4. In the open circuit operation mode, oxygen depletion results in the expected shift in corrosion potential toward more negative values. Δ values are virtually unchanged throughout the exposure period, increasing by only 0.08 degrees after 1350 minutes. The value of ψ similarly is constant during the first 100 minutes or so of exposure, but then increases during a period where the rate of potential change appears to increase. Overall, ψ is increased by 0.260 over the exposure period.

When the specimen potential was fixed at a value corresponding to the most negative potential attained during deaeration of the solution (-400 mV SHE), Δ and ψ were virtually unchanged during the first 50 minutes or so while the cathodic current was decreasing by an order of magnitude. Both Δ and ψ then varied simultaneously in a direction that earlier studies[8] had shown were characteristic of surface roughening. Net change in Δ and ψ were -0.60 and +0.38, respectively.

We can infer from these data on the effect of deoxygenation on the protective films on 304 stainless steel that when initially exposed to a deoxygenated solution when the potential is changing slowly (9.4 mV/minute), the ellipsometer parameters Δ and ψ are rather constant with only a very slight increase in both parameters being evident. This means very slight thinning or changes in the nature of the film have occurred. Based on the reaction:

$$O_2 + 2H_2O + 4e^- \leftrightarrows 4OH^- \qquad\qquad [1]$$

the overall potential change of -94 mV would correspond to a 6 order of magnitude decrease in oxygen concentration. However, later on where there is a rapid rate of potential change, there is a significant increase

29

in values of ψ after 100 minutes or so, while Δ remains essentially constant. This would appear to indicate a greater change in the nature of the film has occurred, but with still no significant thinning, possibly as a result of the decrease in supply of available oxygen as evidenced by the constancy of Δ. Since micropits were observed at this stage, such behavior indicates a localized breakdown in passivity.

Placing the specimen under potentiostatic control at a potential where cathodic reduction of oxygen would be enhanced also accelerates those processes which are characterized by changes in the ellipsometer parameters. The abrupt change in ψ which occurs after about 30 minutes and is followed 20 minutes later by a decrease in Δ could be due to surface roughening. As before, the observation of micropits on the surface of the specimen upon later visual examination confirmed this conclusion.

At this point, our results are in agreement with those recently published by Bates[10] where he correlated various crevice processes to breaks in potential-time curves. However, our ellipsometric studies suggest that, contrary to Bates' proposal, depletion of oxygen alone does _not_ lead to uniform film thinning and loss of passivity over the whole surface, a behavior characteristic of crevice corrosion attack, but instead results in a discrete change in the nature of the film followed by a localized loss of passivity that is more characteristic of pitting.

Effect of the Crevice

As shown in the past section, oxygen depletion alone does not lead to the general attack observed under crevices. The next series of experiments were directed at looking at the role of the crevice. Results from

30

these studies in which a crevice was introduced for the open circuit and potentiostated modes are shown in Figs. 5 and 6. For the open circuit mode several observations are apparent. Concurrent with a slow shift in potential to more negative values, there is a significant decrease in Δ values ($\delta\Delta = \sim0.3°$). Although the value of ψ appears to fluctuate and was not particularly reproducible, there was a general increase in ψ values during the course of exposure ($\delta\psi = \sim0.7°$). After a period of 20-45 minutes, Δ began to increase steadily, reaching a maximum value ($\delta\Delta = \sim2.4°$) in 200-300 minutes, after which it decreased markedly. At this time, several gas bubbles were clearly visible behind the glass plate and a discoloration was apparent at the periphery of the specimen surface.

When potentiostated at the initial immersion corrosion potential (+42 mV), Δ values again decreased markedly during the first 20 minutes of exposure ($\delta\Delta = \sim-0.12°$) before increasing to a maximum value ($\delta\Delta = +.60°$), after about 1450 minutes. The ψ values, however, decreased regularly during the first 200 minutes ($\delta\psi = =0.65°$) then increased for the remainder of the exposure period. Current values slowly increased from +0.66 μA to a final value of 300 μA at the end of the run. The major increase in the current, which indicates an increase in corrosion rate occurred at about the same time as the Δ values started to decrease sharply.

It is obvious from both the open circuit and potentiostatic experiments that completely different optical results are obtained when a crevice is introduced. Although the process of oxygen depletion is probably accelerated within the low volume crevice, the initial direction of change of both Δ and ψ is opposite to that observed in oxygen depletion

31

studies where a crevice was not present, at least for the open circuit experiments (great fluctuations in ψ values for the potentiostates crevice system make any concise analysis impossible at this time).

Before attempting to interpret the ellipsometric observations, it is necessary to discuss the effect of the glass plate on the ellipsometric observations. Since the glass plate is a dielectric there will be no phase change with transmission through the glass plate and the Δ measured will not differ from that resulting from optical conditions at the metal surface. The value of ψ measured, however, will be changed due to the transmission coefficients at the surfaces of the glass plate. These transmission coefficients will in turn depend upon the refractive index of the solution in the crevice. This latter is generally unknown and changing during the course of our experiment.

We sought to determine empirically the effect of increase of the solution refractive index on Δ and ψ outside of a crevice. To do this we made measurements on a stainless steel surface, with a crevice, in both 1N NaCl and 2.5N NaCl solutions, the latter having a higher refractive index. As Table I shows that the measured value of Δ with the crevice in place decreased markedly in value in the more concentrated solution. The value of ψ increased

slightly. Thus, based on the changes in Δ shown in Figs. 5 and 6, the initial stages of crevice corrosion are consistent with and increase in crevice solution index of refraction, i.e., an increase in the concentration of Cl^- and metallic ions. Because ψ is difficult to interpret in the presence of a crevice for the reasons given above and because of the greater fluctuations in the values measured, we cannot judge whether the ψ measurements are indicative of crevice solution concentration during the first part of the chain of events leading to crevice corrosion.

The substantial increase in Δ and continued decrease in ψ following the first phase is consistent with an overall decrease in thickness of the protective surface film. Since oxygen depletion alone has been shown not to produce such an effect, we can assume that such thinning results from whatever happened during the first phase of the process, where Δ was observed to decrease . Finally, the marked decrease in Δ is in the same direction as was previously noted for the non-crevice oxygen depletion studies, and is characteristic of surface roughening and/or film growth. Notably, this decrease comes at the same time that the current measurements indicate an increased rate of corrosion.

The effect of a crevice on the corrosion rate and ellipsometer parameters of the Ti 8-1-1 alloy is shown in Fig. 7. This alloy, which is not susceptible to crevice corrosion in this environment at room temperature, exhibits none of the ellipsometric variations associated with the onset of crevice corrosion attack on 304 stainless steel when potentiostated at the open circuit corrosion potential. In fact, Δ, ψ, and i are relatively constant over the entire period of exposure.

Although these mechanistic inferences are consistent with the observed ellipsometric variation, they are by no means the only possible interpretation. This is so because the ellipsometric measurements reflect average overall changes occurring under the glass plate. In other words, one process - i.e., solution concentration - could easily mask out small changes in the film/metal substrate. Much further work is necessary to make ellipsometric observations of crevices more definitive and quantitative. However, the results just described are important qualitatively because they indicate the times at which changes occur in the crevice in the processes leading to crevice attack. Moreover, a reasonable picture, consistent with the optical measurements of what events are initiated during these changes can be developed using measurements in special environments without a crevice. This sequence of events for the susceptible stainless steel exposed to a crevice in a chloride solution can be summarized as follows:

1. Depletion of dissolved oxygen within the confines of the crevice accompanied by a build-up in concentration of dissolved metal and chloride ion. (Slight film dissolution resulting from the consumption of hydrogen ion generated by metal ion hydrolysis is probably masked in these ellipsometer measurements.)

2. Overall film thinning which probably continues to consume hydrogen ions, accompanied by increased metal dissolution.

3. A sharp decrease in pH when the protective film is gone, accompanied by surface roughening as metal dissolution proceeds into the final stages of crevice corrosion attack. C thodic reduction of H^+ could also be expected to occur.

In contrast, for the non-susceptible Ti alloy, a constancy of ellipsometric and current measurements over the entire exposure period indicate that none of the crevice solution concentration effects which were detected for the susceptible 304 stainless steel had occurred.

This study has thus shown that it is feasible to study crevice corrosion by means of ellipsometry. It has demonstrated a difference in the optical behavior between a metal susceptible to crevice corrosion (304 stainless steel) and one that is not (Ti 8-1-1). It has been shown capable of detecting a number of stages leading to crevice attack. Much further work remains, however, to enable us to develop the technique into a more quantitative tool. Future work will also involve modifying the technique to enable pH and potential measurements to be made within the crevice.

REFERENCES

1. R. J. Landrum, Chemical Engineering 118, 24 (1969).

2. S. K. Coburn, Materials Protection 6, 33 (1967).

3. D. A. Vermilyea and C. S. Tedman, Jr., J. Electrochem. Soc. 117, 437 (1970).

4. W. D. France, Jr., "Localized Corrosion - Cause of Metal Failure," ASTM Special Technical Publication 516, M. Henthorne, Chairman, Atlantic City, 1971 (ASTM, Philadelphia), p. 164.

5. I. L. Rosenfeld and I. K. Marshakov, Corrosion 20, 115t (1964).

6. R. B. Mears and U. R. Evans, Trans. Faraday Soc. 30, 417 (1934).

7. U. R. Evans, J. Inst. Metals 30, 239 (1923).

8. J. Kruger, Corrosion 22, 88 (1966).

9. J. R. Ambrose and J. Kruger, Corrosion 28, 30 (1972).

10. J. F. Bates, Corrosion 29, 28 (1973).

TABLE I

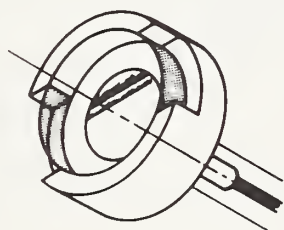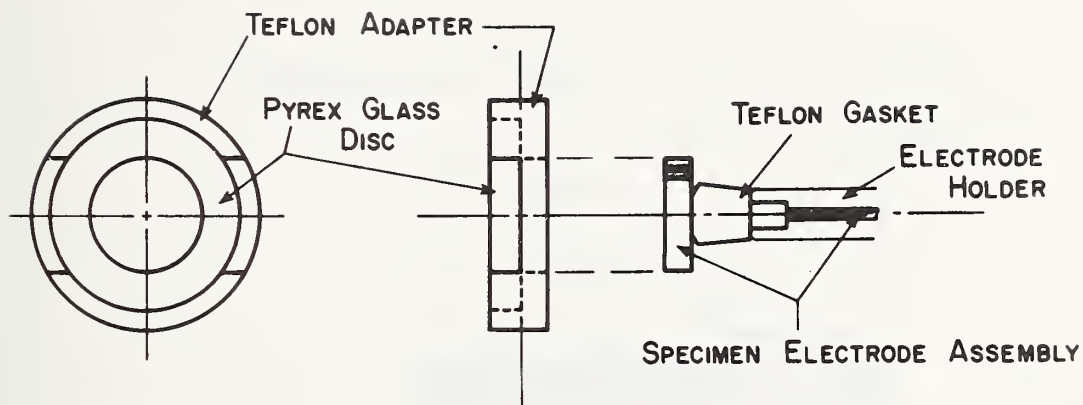| NaCl Solution Concentration	Refractive Index	Δ	ψ	$\delta\Delta_{1.0\rightarrow2.5}$	$\delta\psi_{1.0\rightarrow2.5}$
1.0N	1.3432	113.86	29.38	-	-
2.5	1.3567	111.70	29.41	-2.16°	+.03°

Figure 1   Schematic of the Teflon adapter and glass disc used to simulate
a crevice where ellipsometer measurements could be made.
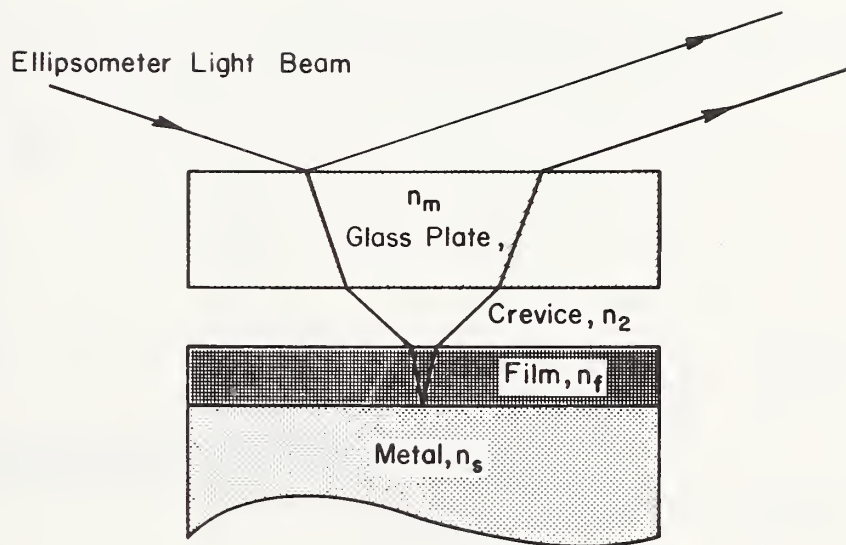
Figure 2   Model of the crevice system showing refraction of ellipsometrically
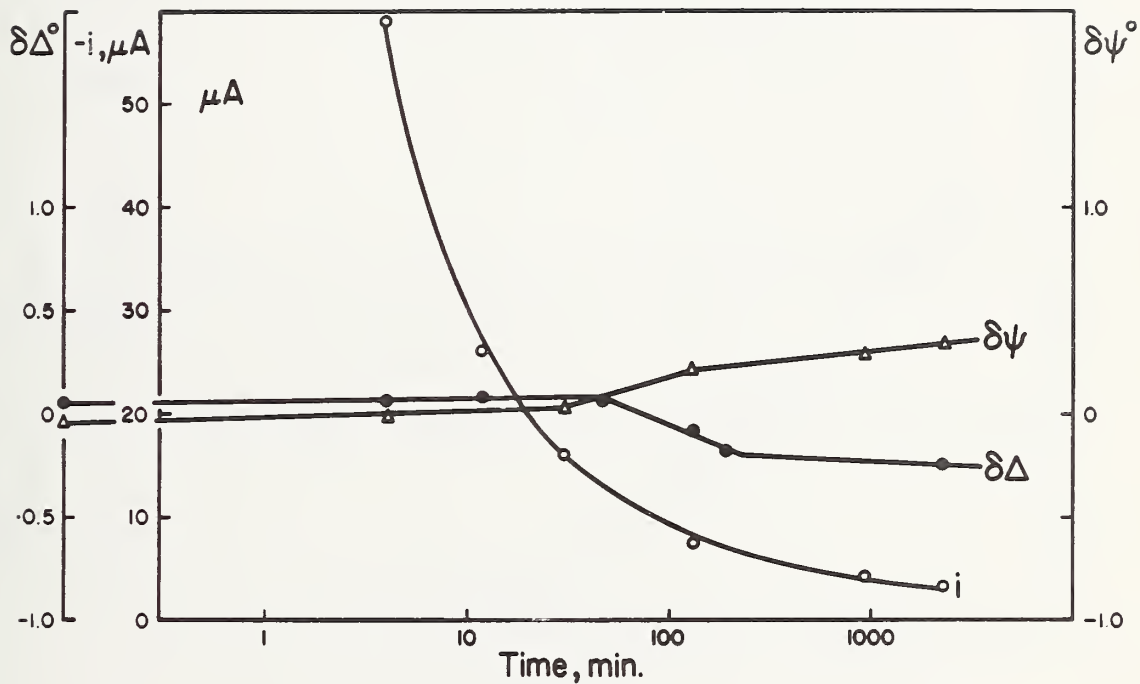   polarized light in various media.

Figure 3   Effect of solution deoxygenation on ellipsometer parameters
            Δ and ψ, and the corrosion current, as a function of $\log_{10}$
            time for 304 stainless steel with no crevice in 1.0N NaCl.
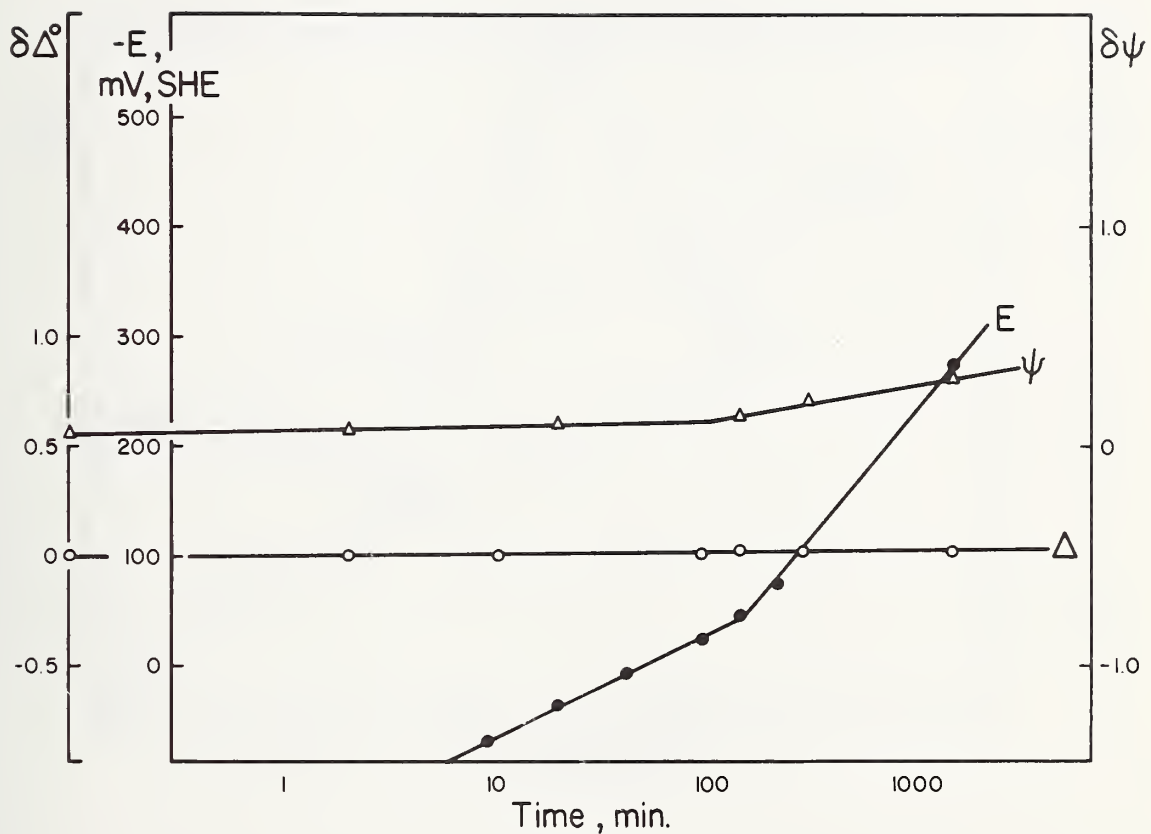   Specimen is potentiostated at -400 mV SHE.

Figure 4   Effect of solution deoxygenation on ellipsometer parameters
Δ and ψ, and the corrosion potential, as a function of $\log_{10}$
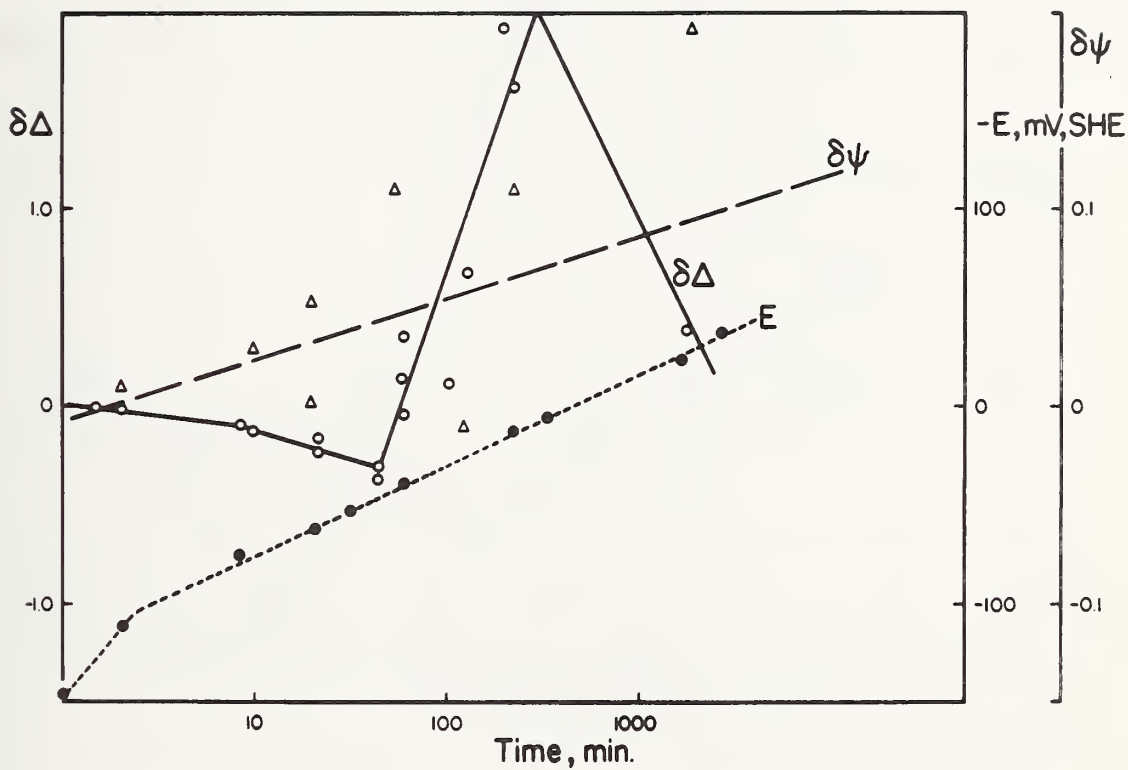time for 304 stainless steel with no crevice in 1.0N NaCl.

Figure 5   Effect of a crevice on ellipsometer parameters Δ and ψ, and the corrosion potential, as a function of $\log_{10}$ time for 304 stainless steel in 1.0N NaCl.
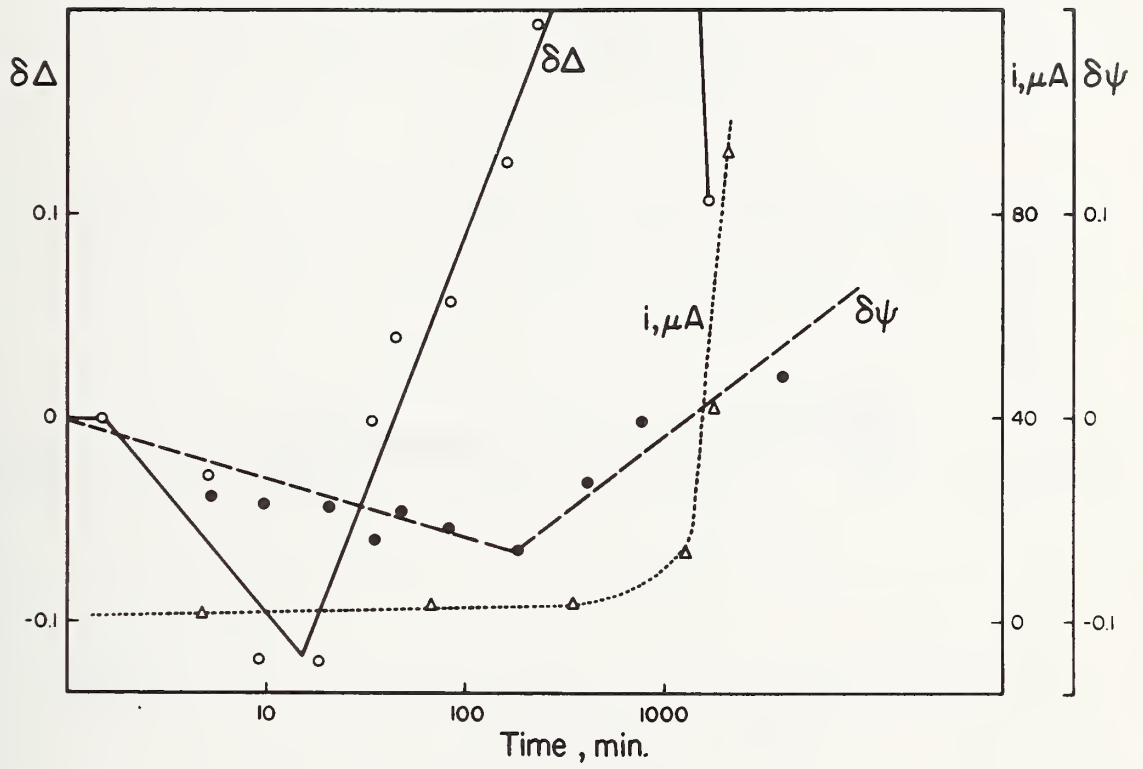
Figure 6   Effect of a crevice on ellipsometer parameters Δ and Ψ, and the corrosion current as a function of $\log_{10}$ time for 304 stainless steel in 1.0N NaCl; specimen is potentiostated at +42 mV SHE.
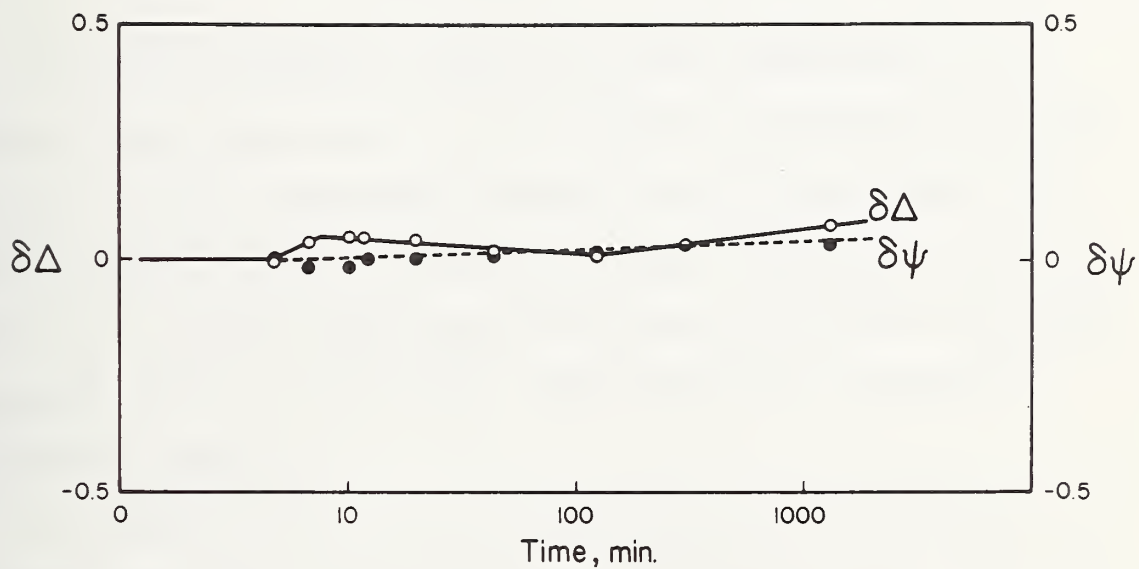
43

Figure 7   Effect of a crevice on ellipsometer parameters Δ and ψ as a function
           of $\log_{10}$ time for Ti 8-1-1 alloy in 1.0N NaCl; specimen is
           potentiostated at +169 mV SHE.

Part III. To be submitted to the Journal of the Electrochemical Society

TRIBO-ELLIPSOMETRIC STUDY OF THE REPASSIVATION KINETICS
OF A TI 8AL-1MO-1V ALLOY

J. R. Ambrose and J. Kruger
Institute for Materials Research
National Bureau of Standards
Washington, D.C. 20234

ABSTRACT

The tribo-ellipsometry technique with which measurements of film growth and total reaction rate are made following film removal by abrasion was used to determine repassivation kinetics and stress corrosion cracking (SCC) susceptibility for Ti-8Al-1Mo-1V alloy. Repassivation transient behavior in a 1.0N NaCl solution, where cracks have been found to propagate, was compared to that in a 1.0N $NaNO_3$ solution where SCC susceptibility has never been detected.

Film growth kinetics in both solutions were consistent with a Fleischmann-Thirsk mechanism of oxide patch nucleation and two-dimensional growth, although the film growth rate was significantly slower in the 1.0N NaCl solution. This was in turn responsible for an increase in metal dissolution in a solution where crack propagation velocities have been measured, but at an apparent rate slower than necessary to propagate such cracks by metal dissolution alone.

TRIBO-ELLIPSOMETRIC STUDY OF THE REPASSIVATION KINETICS

OF A TI 8AL-1MO-1V ALLOY

J. R. Ambrose[*]and J. Kruger
Institute for Materials Research
National Bureau of Standards
Washington, D.C. 20234

Theoretical treatments of the relationship between repassivation kinetics and susceptibility to stress corrosion cracking have recently been incorporated into mechanisms for cracking of a number of materials, noticeably mild steel[1] and titanium alloys.[2] Studies by Beck[2] relating crack propagation velocities to anodic current densities measured following fast fracture of titanium alloy wire utilized an empirical relationship to estimate film growth rates during the repassivation transient.

The recently developed technique of tribo-ellipsometry, with which a determination of both anodic current and film growth rates can be made following passive film removal by abrasion, makes possible a separation of the total repassivation process into film growth and metal dissolution components.

This work describes the results of a study comparing repassivation behavior of a commercial titanium alloy (Ti 8Al-1Mo-1V) exposed in a solution where cracks are known to propagate (1.0N NaCl) and in 1.0N NaNO$_3$, where no susceptibility to cracking has been detected.

An attempt has been made to correlate measured film growth rates with the Fleischmann-Thirsk patch nucleation and growth mechanism and to estimate crack propagation velocities which would result from metal dissolution during repassivation.

---

[*]A portion of this work has been included in the research dissertaiton submitted to the University of Maryland in partial fulfillment of the requirements for the Ph.D. degree.

EXPERIMENTAL

The description of the experimental apparatus and technique of tribo-ellipsometry has been presented in prior publications.[3,4]

A Ti 8Al-1Mo-1V commercial alloy was used in this study: 1.905 cm diameter x 0.635 cm thick cylindrical specimens were machined from rod stock and polished with silicon carbide metallographic papers followed by rotary polishing on nylon cloth with 6μ diamond paste. Air-saturated solutions of 1.0N NaCl and 1.0N $NaNO_3$ were prepared from ACS reagent grade chemicals and distilled water.

Specimen potentials were controlled potentiostatically, with the repassivating current pulse generated upon cessation of abrasion used to trigger the sweep of a dual channel oscilloscope which also recorded the output of the photometer system used to monitor changes in ellipsometer light intensity.

Total coulombs, Q_T, passed during the transient were determined by graphical integration of the total current, i_T; film thickness, x, was determined from light intensity changes which were converted using pre-determined calibration data.

THE REPASSIVATION RATIO, R_p

Although measurement of the total current, i_T, and the film thickness, x, as a function of time during the repassivation transient is relatively straightforward, several uncertainties exist that make it difficult to render the data completely unambiguous and quantitative in any treatment of data obtained utilizing this technique. These uncertainties are as follows:

47

1. The total current involved in repassivation, i_T, is the current supplied by the potentiostat to maintain the specimen potential at some fixed value with respect to a reference electrode potential. If any cathodic reduction were also to supply current, a determination of i_a, the anodic current used during repassivation, becomes difficult. Of course, i_c can be made negligible by operating at potentials 50 mV or so more positive than the open circuit or corrosion potential

this would defeat the point of attempting to predict susceptibility to SCC for materials immersed in specific environments.

2. The charge utilized in the formation of an oxide film is given by

$$Q_x = {}_0\!\int^t i_x dt = \frac{zF\rho Ax}{M} \qquad [1]$$

where i_x = current consumed by film formation

   z = valence, $\dfrac{\text{equivalents}}{\text{mole}}$

   F = Faraday's constant, $\dfrac{\text{coulombs}}{\text{equiv}}$

   ρ = density of oxide, $\dfrac{\text{gms}}{\text{cm}^3}$

   A = surface area of oxide layer, cm^2

   x = film thickness, cm

   M = molecular weight of oxide, $\dfrac{\text{gms}}{\text{mole}}$

It is difficult to know the value of area, A, for the surface where film growth (and metal dissolution) occurs since the efficiency of the abrasion process is difficult to ascertain.

To get around these difficulties a recent paper[5] expressed the experimentally measured variables of total current, i_T, and film thickness, x, in the form of a ratio, designated R_p and given by:

48

$$R_p = \frac{_0\int^t i_T dt}{x} \qquad [2]$$

Since $_0\int^t i_T dt = Q_T$ and $x = \frac{M}{zF\rho A} Q_x$ then

$$R_p = \frac{Q_T}{kQ_x} \qquad \text{where } k = \frac{M}{zF\rho A} \quad . \qquad [3]$$

If we assume that $Q_T = Q_x + Q_d$ then

$$R_p = \frac{Q_x + Q_d}{kQ_x} = \frac{1}{k}[1 + \frac{Q_d}{Q_x}] \qquad [4]$$

where Q_d = charge consumed by metal dissolution.

Although evaluation of A is difficult, it is sometimes useful to express R_p as a dimensionless variable, designated R_p^* and equal to

$$1 + \frac{Q_d}{Q_x} \qquad [5]$$

since results would be independent of the particular experimental procedures and apparatus employed. Although R_p and R_p^* differ in magnitude only by the constant, k, R_p values are determined directly from experimental measurements; therefore, discussion and conclusions will be based on R_p values. Differentiating R_p with respect to time

$$\frac{dR_p}{dt} = \frac{1}{k}\left[\frac{Q_x \frac{dQ_d}{dt} - Q_d \frac{dQ_x}{dt}}{Q_x^2}\right] \qquad [6]$$

$$= \frac{1}{k}\left[\frac{Q_x i_d - Q_d i_x}{Q_x^2}\right] \qquad [7]$$

$$= \frac{1}{k}\left(\frac{i_d}{Q_x}\right) - \frac{1}{k}\left(\frac{Q_d i_x}{Q_x^2}\right) \qquad [8]$$

49

In this derivation we have neglected the cathodic current, i_c. This is not an unreasonable assumption since it is generally quite low except in acid solutions, hence negligible compared to i_a when the anodic overvoltage is high.

The values of R_p and $\frac{dR_p}{dt}$ can be used to distinguish between metal dissolution and film repair and thus provide a parameter for predicting stress corrosion cracking susceptibility. As an example, consider the various limiting cases:

Case I: $i_d \gg i_x$

    i. R_p becomes very large and i_x is nearly 0.

    ii. $\frac{dR_p}{dt} > 0$

This would correspond to a situation where general corrosion without any repassivation was occurring.

Case II: $i_x \gg i_d$

    i. $R_p \simeq \frac{1}{k}$

    ii. $\frac{dR_p}{dt} \simeq -\frac{1}{k}\left(\frac{Q_d i_x}{Q_x^2}\right)$; from eq. [8]

This corresponds to virtually instant repassivation with no metal dissolution and little susceptibility to SCC.

Case III: $i_x \simeq i_d$

    i. $R_p = k\left(1 + \frac{Q_d}{Q_x}\right)$

    ii. $\frac{dR_p}{dt} \simeq 0$

    ii. $x > 0$

Subcase IIIa: $\frac{dx}{dt} > 0$; (at large values of t).

In this case, the film formed is not protective, but is similar in characteristics to Case I because general corrosion or pitting results.

Subcase IIIb: $\frac{dx}{dt} \simeq 0$; (at large values of t).

These conditions would be those most consistent with the initiation and propagation of stress corrosion cracks based on a metal dissolution mechanism which is dependent upon the rate of repassivation. In other words, a relatively large value of R_p, with small value of $\frac{dR_p}{dt}$ and $\frac{dx}{dt}$ indicate that metal dissolution accompanies film regrowth, but that repassivation eventually occurs, thus protecting the walls of the advancing crack and restricting propagation of the crack to the area directly at its tip.

These conditions are summarized in Table I.

RESULTS

1. Effect of Anions

Results of the tribo-ellipsometric repassivation kinetics experiments conducted in 1N NaNO$_3$ and 1N NaCl solutions at respective corrosion potentials* are shown in Figs. 1 and 2. The value of the repassivation ratio, R_p, is significantly higher in the NaCl solution, approaching a limiting value of about 2 $\frac{mcoul}{nm}$ when monolayer coverage of 0.3 nm is obtained as compared to the NaNO$_3$ solution ($R_{p_{lim}} \simeq 0.3 \frac{mcoul}{nm}$). The values of the ellipsometrically determined film thickness are also shown. In NaNO$_3$, an oxide thickness of 0.30 nm is present on the metal surface by the time the abrasion wheel had retracted to allow ellipsometric measurements

---

*Although corrosion potentials are extremely difficult to reproduce, depending upon specimen surface treatment and history[6], the open circuit potential established for the particular specimen used in these studies after several abrasion cycles was the same for Ti 8-1-1 in both solutions used and was fairly reproducible even when the specimen was repolished or solutions changed.

51

($\sim$ 5 msec.), indicating extremely rapid early stage film growth. In NaCl, on the other hand, film growth is so slow that a film thickness of 0.30 nm is not reached until 38 msec. following cessation of abrasion.

2. Effect of Potential

The results of repassivation experiments conducted in the 1N $NaNO_3$ and 1N NaCl solutions at a higher anodic potential (+706 mV SHE) are given in Figs. 3 and 4. $R_{p_{lim}}$ values are significantly higher than at open circuit in both solutions ($\sim$3.00 for NaCl; $\sim$1.02 for $NaNO_3$). Initial film thickness growth is substantially slower at +706 mV than at -222 mV for the $NaNO_3$ solution. A comparison of oscilloscope tracings for Ti 8-1-1 in 1N NaCl and 1N $NaNO_3$ at 706 mV SHE is given in Fig. 5.

Peak current densities for the transients in NaCl and $NaNO_3$ were 65.0 and 18.8 mA, respectively.

Film growth kinetics were determined and are not inconsistent with a parabolic growth law - i.e., a straight line was obtained when film thickness was plotted against the square root of time. These plots for Ti 8-1-1 in 1N NaCl and 1N $NaNO_3$ at both potentials are given in Fig. 6. The values of R_p, R_p^*, T_m (the time required for obtaining 0.30 nm film thickness), $dx/d(t^{1/2})$, and i_{max} are given in Table II.

DISCUSSION

1. Repassivation Ratio and Stress Corrosion Susceptibility

From Fig. 1 and Table II it can be seen that for Ti 8-1-1 in 1N $NaNO_3$ at the corrosion potential of -222 mV SHE, a low value of R_p with $dR_p/dt \approx 0$ was maintained throughout the repassivation transient. Based on the size of the oxide ion a monolayer of TiO_2 would be approximately

52

0.30 nm in thickness; it formed in <5 msec. in this environment. These results are characteristic for a Case II repassivation transient in which most of the current transient is utilized in rapid film growth without significant metal dissolution. When this is compared to the results obtained in 1N NaCl at the same potential, where crack propagation velocities on the order of $10^{-2} \frac{cm}{sec}$ have been measured,[2,7] it is seen that R_p is significantly higher as is dR_p/dt indicating substantial metal dissolution which can be accounted for by low rates of film growth in 1N NaCl. Although monolayer coverage is not obtained until 38 msec. following cessation of abrasion, R_p changes slope at about 12 msec., indicating some inhibition of metal dissolution, perhaps by formation of a precipitated salt layer on the surface resulting from saturation of the diffusion layer with $TiCl_3$ (Fig. 2). At any rate, repassivation is eventually achieved (Case IIIb). Similarly, at an applied potential of +706 mV SHE, R_p is quite high in the chloride solution with R_p changing slope at about 10 msec. which would substantiate a precipitated salt passivation mechanism since a saturated solution of $TiCl_3$ would be obtained more rapidly at these higher current densities. The time to complete monolayer coverage, t_m, is about 20 msec. R_p and dR/dt for 1N $NaNO_3$, although larger than at the lower potential, are far less than the NaCl environment.

Based upon analysis of the R_p, dR_p/dt and t_m parameters, it appears that, at least for titanium alloys, a Case I → Case IIIb transition in dR_p/dt with an initial high R_p predicts susceptibility to stress corrosion cracking under the experimental conditions employed.

We should, nevertheless, not rule out a mechanism based on fracture of titanium hydride (TiH_2) produced by the cathodic reduction reaction:

$$Ti + 2H^+ + 2\bar{e} \rightarrow TiH_2 \qquad\qquad [9]$$
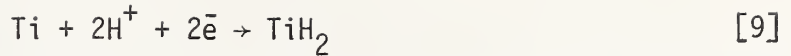
Since the results of our study show lower repassivation rates in the environment known to be susceptible to SCC, repassivation kinetics that can control or limit access of H^+ to the Ti surface may still be relevant. Secondly, the fractography found for titanium alloys that have undergone SCC show a great deal of cleavage.[8]. This could rule out metal dissolution as a factor during crack propagation. However, the significantly higher metal dissolution in Cl^- solutions suggested by Beck[2] and confirmed in this study cannot be ignored. The effect of repassivation on metal dissolution must be important in the initiation stages of a crack when, because the pH of neutral chloride solutions would be near bulk solution values, the H^+ concentration would be too low for the reaction in Eq. 9 to play an important role. During later stages of propagation, where metal ion hydrolysis leads to pH and iR drops within the crack, hydride cleavage mechanisms must be considered in addition to the effects of environmental variations on film growth and metal dissolution kinetics.

2. Film Growth Kinetics

The first stage of film growth appears to be consistent with the Fleischmann and Thirsk analysis of oxide nucleation and growth.[9] They assume an instantaneous nucleation of n patches/cm^2 which spread in 2 dimensions until formation of an oxide monolayer is complete. The equation for the density to the oxide patches is given by [9]:

$$i_f = 2m \, Q_f \, Ct \, \exp[-Ct^2] \qquad\qquad [10]$$

where m = number of monolayers

Q_f = charge density of oxide monolayer, $\dfrac{coulombs}{cm^2}$

54

t = time, seconds

$$C = \pi n \left(\frac{\delta_M i_2}{Q_f} \right)^2 \cdot 2$$

n = number of oxide patches, cm^{-2}

δ_M = thickness of a monolayer, cm

i_2 = current density at periphery of oxide patches, $amperes/cm^2$

Since the patch thickness is assumed constant until complete mono-layer coverage is obtained, Q_f would be constant; C would also be independent of time. This allows integration of Eq. 10 [from (2)]:

$$1 - \theta = \exp [-Ct^2] \qquad [11]$$

where θ is the fraction of surface coverage.

Taking logarithms of both sides gives:

$$\log [1 - \theta] = -Ct^2 \qquad [12]$$

Since θ is proportional to the ellipsometer parameter Δ which depends on average film thickness, hence also to ΔP (the change in polarizer reading), a plot of log ΔP vs t^2 should be linear if the Fleischmann-Thirsk model is an appropriate one. Results are given in Fig. 7.

From Table II, we find that a monolayer (approximately 0.30 nm) has formed on Ti 8-1-1 in the $NaNO_3$ solution at the open circuit potential in less than 5 msec. A comparison with the NaCl solution at the same potential shows that monolayer coverage is not obtained until some 30 msec. later, and the log $(1 - \theta)$ vs t^2 plot is linear, indicating possible applicability of the Fleischmann model. Experiments run at the higher anodic potential give approximately the same effect, that is, film growth is substantially slower in the chloride solution than in the nitrate. The fact that first stage growth rates at the higher potential are lower in the nitrate solution may be due to a localized pH lowering from solvated

55

Ti^{+3} hydrolysis. This could measurably affect film growth kinetics. Such an effect would not be noticeable in the chloride solution where hydrolysis of the metal ions probably results in pH decreases in both potentials. The values of i_{max} for both solutions at the two potentials would substantiate this conclusion. In $NaNO_3$ the relative increase in peak current resulting from film removal at the higher potential is about 6:1 whereas only about a 3:1 increase is noted for chloride solution (Table II).

Simultaneous determination of both film thickness and total current allow an estimate of the amount of metal dissolution occurring during the repassivation transient. Such an estimate would allow prediction of the crack propagation velocities to be expected if propagation proceeds via an electrochemical dissolution mechanism as suggested by Beck.[2]

Assuming that metal dissolution occurs by Tafel kinetics on the bare metal between patches:

$$i_d = i_{d,o} exp \left[\alpha (E_a - E_{o,+})/RT \right] \qquad [13]$$

where $i_{d,o}$ = exchange current density, $\frac{A}{cm^2}$

α = transfer coefficient

E_a = applied potential (potentiostat)

$E_{o,+}$ = equilibrium potential for dissolution reaction.

Total metal dissolution current over the entire surface is proportional to the area of bare metal exposed. It can be assumed, however, that the local dissolution current density on bare metal surfaces remains constant over the span of the repassivation transient until the patches coalesce. This would allow an estimate of the maximum penetration of metal by electrochemical dissolution. Since the local dissolution current density is given by i_{max}/A, $x_{p_{max}}$, the maximum penetration at those areas of surface last

covered by the monolayer, is given by:

$$x_{p_{max}} = \frac{i_{max} M}{zF\rho A} t_m \qquad [14]$$

where M = atomic wt. of metal, $\frac{gm}{g - a}$

z = valence, $\frac{equiv}{g - a}$

ρ = density of metal, gms/cm^3

A = initial bare surface area produced, cm^2

F = Faraday's constant, $\frac{coul}{equiv}$

t_m = time for monolayer formation, sec.

Using data from Table I for Ti 8-1-1 in 1N NaCl at the open circuit potential of -222 mV SHE, we obtain a value of $x_{p_{max}}$ of 2.3×10^{-7} cm or a maximum propagation velocity of 6.0×10^{-6} cm/sec. Even if the $i_{t_{max}} \simeq i_d$ approximation is in error due to localized cathodic reactions, as well as overestimating bare metal surface area, propagation velocities based on electrochemical metal dissolution do not come close to the observed stress corrosion crack propagation velocities of 8×10^{-3} cm/sec by Beck at this potential.[2]

However, penetration velocities are potential dependent, $v_{p_{max}}$ being calculated as 16.2×10^{-6} cm/sec at a potential of +706 mV SHE. From this we would predict that upon increasing the applied potential by 1 volt the propagation velocity would increase by a factor of three, in agreement with Beck.[2] This would suggest that although metal dissolution does not account for the observed crack propagation rates, it may be a necessary condition for such propagation.

The Fleischmann-Thirsk model for patch growth, coupled with the assumption of constant metal dissolution current density at the metal surface, would, however, predict creation of localized penetration sites. The geometry of these sites would lead to increased stresses at the point of maximum penetration as well as effecting environmental composition variations due to the occluded nature of these sites (Fig. 8).

Whether crack propagation then proceeds via a dissolution assisted mechanical cleavage process or by fracture of a brittle region produced by entry into the metal of hydrogen formed by cathodic reduction cannot be determined on the basis of the results presented here. The specific function of halide ions (e.g., Cl^-) in restricting lateral oxide growth is also highly speculative but may result from preferred ion adsorption inhibiting oxide growth kinetics. Green and Sedricks suggest that on the basis of their ellipsometric potential step experiments film growth kinetics play no part in determining SCC.[7] However, they did not study film growth kinetics on bare metal surfaces, making their conclusions somewhat irrelevant to stress cracking. By varying the water content of 3.5% LiCl in dimethyl sulfoxide solutions they have been able to control crack propagation velocities in Ti 8-1-1.[10] Their results suggest the possibility of a hydrogen embrittling mechanism since no available hydrogen is present in pure DMSO; however, neglect in measuring their solution conductivities leaves open the possibility of crack propagation rates being limited by mass transfer of some rate determining species. On the other hand, this work indicates that film growth rate and SCC susceptibility appear to be related for those environments studied.

- 58 -

CONCLUSIONS

1. Ti 8-1-1 alloy repassivates rapidly in $NaNO_3$ solution as indicated by a low R_p and dR_p/dt with a monolayer of oxide being formed in less than 5 msec.

2. Ti 8-1-1 alloy repassivates less rapidly in NaCl solution than in $NaNO_3$ solution as indicated by a higher R_p with an initially higher dR_p/dt. Although monolayer coverage is not obtained until 38 msec. following oxide removal, a decrease in dR_p/dt is observed at 12 msec., probably to inhibition of metal dissolution by a precipitated salt layer.

3. An analysis of ellipsometrically determined film growth kinetics on Ti 8-1-1 shows that the Fleischmann-Thirsk model of oxide patch nucleation and growth is applicable in both 1N NaCl and 1N $NaNO_3$ solutions.

4. A calculation of the maximum penetration resulting from Ti dissolution in Ti 8-1-1 in NaCl solution during the 38 msec. time interval for oxide monolayer formation shows that crack propagation velocities observed by others cannot be accounted for by metal dissolution alone.

ACKNOWLEDGEMENT

REFERENCES

1. T. P. Hoar & J. R. Galvele, Corrosion Sci. $\underline{10}$, 211 (1970).

2. T. R. Beck, "The Theory of Stress Corrosion Cracking in Alloys,"
    J. C. Scully, ed., NATO Scientific Affairs Division, Brussels (W. S.
    Maney, Leeds, 1971), p. 64.

3. J. R. Ambrose and J. Kruger, Corrosion $\underline{28}$, 30 (1972).

4. J. Kruger et al, National Bureau of Standards Report No. 10-876,
    Technical Summary Report No. 3, Contract NAONR 18-69, NR 036-082, 1972.

5. J. R. Ambrose & J. Kruger, Proc. 5th Int. Cong. Met. Corr., Tokyo, 1972, in
    print.

6. T. R. Beck, J. Electrochem. Soc. $\underline{114}$, 551 (1967).

7. J. A. S. Green and A. J. Sedricks, Metall. Trans. $\underline{2}$, 1807 (1971).

8. J. C. Scully, "The Theory of Stress Corrosion Cracking in Alloys,"
    J. C. Scully, ed.,(NATO Scientific Affairs Division, Brussels, 1971),
    p. 127.

9. M. Fleischmann and H. R. Thirsk, Advances in Electrochemistry and
    Electrochemical Engineering $\underline{3}$, (Interscience, New York, 1963),
    p. 123.

10. J. A. S. Green and A. J. Sedricks, Corrosion $\underline{28}$, 220 (1972).

11. H. H. Uhlig, Proc. Int. Cong. Fundamental Aspects of Stress Corrosion
    Cracking, Ohio State University, 1967 (NACE, Houston, 1969), p. 93.

Table I.   Prediction of Type of Corrosion Process from Measured Repassivation Parameters

Repassivation Parameter				Significance
R_p^*	dR_p/dt	x	dx/dt	
>1	≥ 0	≈ 0	≈ 0	Case I: $i_d >> i_x$; very little film growth; general corrosion attack.
≈ 1	≤ 0	>0	≈ 0	Case II: $i_x >> i_d$; most of current goes into formation of film; characteristic of the passive state.
>1	≥ 0	≥ 0	≥ 0	Case IIIa: $i_x \approx i_d$; film which forms either is not protective (similar to Case I) or grows too slowly to cover the surface, characteristic of general attack or pitting
>1	≤ 0	>0	≈ 0	Case IIIb: $i_x \approx i_d$; characteristic of a system which has eventually passivated after some metal dissolution has occurred. This would correspond to a system where the metal dissolution/film rupture model would apply.

Table II. Repassivation Parameters for Ti 8-1-1 Alloy in 1N NaNO$_3$ and 1N NaCl Solutions

Solution	Potential, mV SHE	$R_p(t_m)^1$, $\frac{mcoul}{nm}$	$R_p*(t_m)^2$	t_m,msec	$(\frac{dR_p}{dt})t<t_m$, $\frac{mcoul}{nm\ msec}$	$(\frac{dR_p}{dt})t>t_m$, $\frac{mcoul}{nm\ msec}$	$(\frac{dx}{dt}1/2)t<t_m$, $\frac{nm}{msec}1/2$	$(\frac{dx}{dt}1/2)t>t_m$, $\frac{nm}{msec}1/2$	i_{max} ma
1N NaNO$_3$	-222	0.3	1.04	< 5	——	+0.005	——	0.0350	4.2
1N NaCl	-222	2.0	6.94	38	+0.130	+0.004	0.0150	0.0405	24.0
1N NaNO$_3$	+706	1.0	3.47	20	+0.052	+0.006	0.0167	0.052	18.8
1N NaCl	+706	3.0	10.4	20	+0.174	-0.005	0.0272	0.072	65.0

[1]Good reproducibility was obtained for reported R_p values with a relative precision of less than ±5% being obtained for all measurements. This leads, for example, to a maximum range of ±0.2 mcoul/nm in the R_p determination for Ti 8-1-1 in 1N NaCl at +706 mV SHE.

[2]The R_p* values reported in Table IV are based upon an approximate area of bare metal produced during abrasion of 0.14 cm². This value of area was computed by assuming that $i_T \approx i_x$ after monolayer coverage on Ti 8-1-1 in 1N NaNO₃ solution, when metal dissolution can be assumed low. Hence,

$$\int_{t_1}^{t_2} i_{T} dt \approx q_x = \frac{zF\rho Ax}{M} \; ; \; \text{or} \; A \approx \frac{M_{t_1}\int^{t_2} i_T dt}{zF\rho x}$$
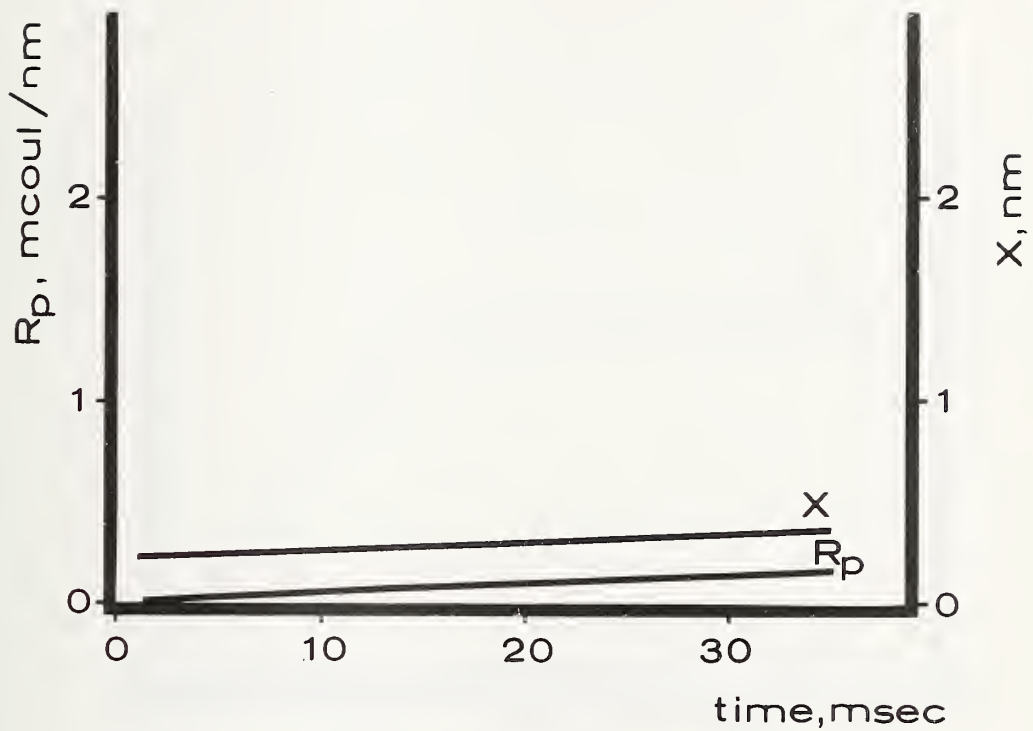
Fig. 1. Change in thickness, x, and repassivation ratio, R_p, after removal of the abrasion wheel of the tribo-ellipsometric apparatus for Ti 8-1-1 in 1N NaNO$_3$ at 25°C. The alloy is at the open circuit (corrosion) potential -222 mV (SHE).
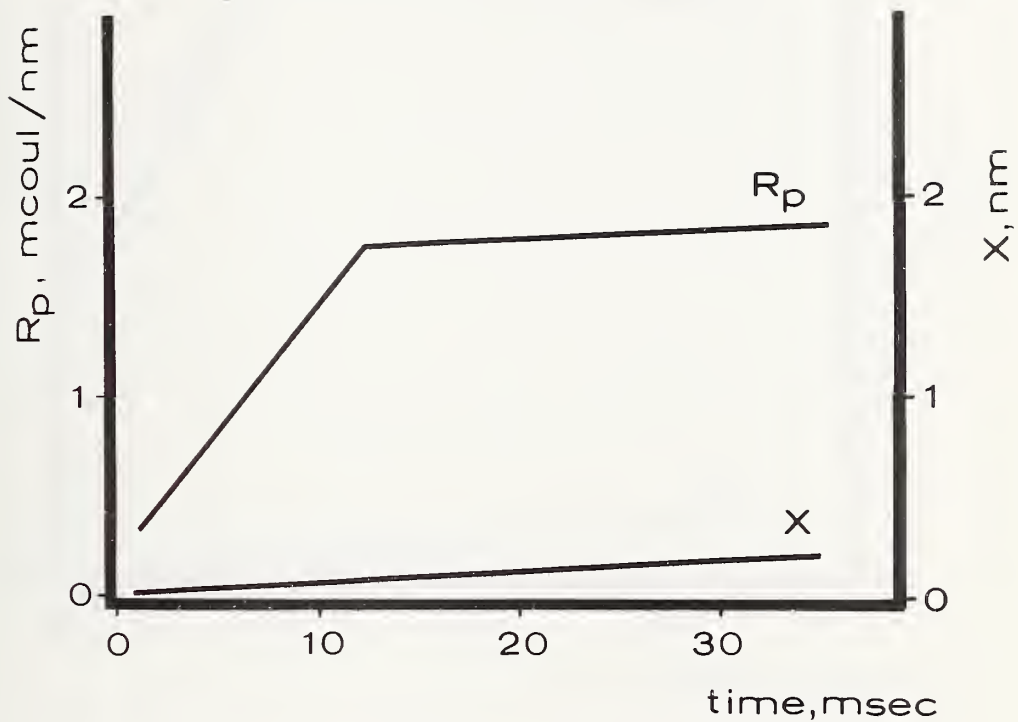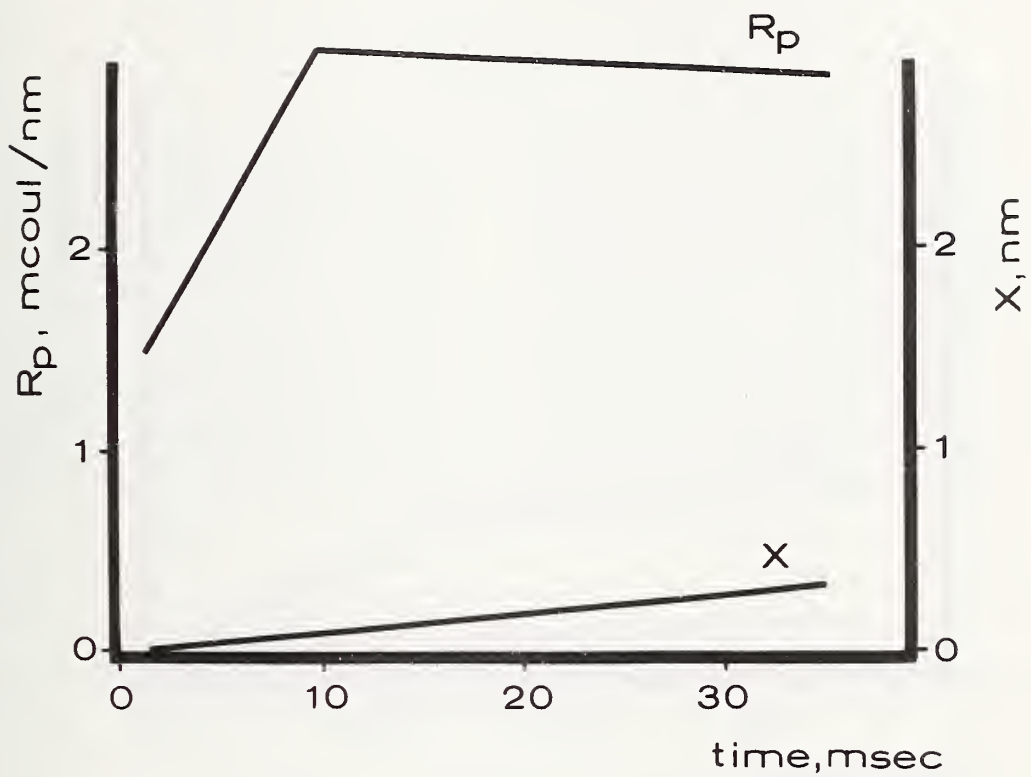
Fig. 2. Change in thickness, x, and repassivation ratio, R_p, after removal of the abrasion wheel of the tribo-ellipsometric apparatus for Ti 8-1-1 in 1N NaCl at 25°C. The alloy is at the open circuit (corrosion) potential -222 mV (SHE).

Fig. 3. Change in thickness, x, and repassivation ratio, R_p, after removal of the abrasion wheel of the tribo-ellipsometric apparatus for Ti 8-1-1 in 1N NaCl at 25°C. The alloy is at +706 mV (SHE).
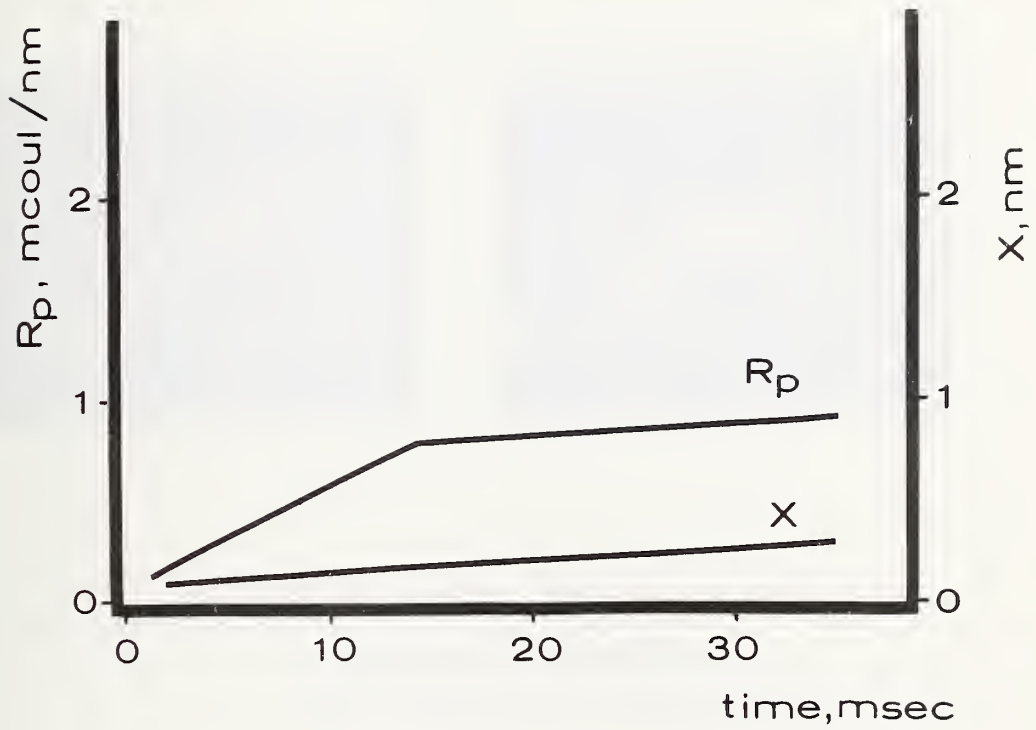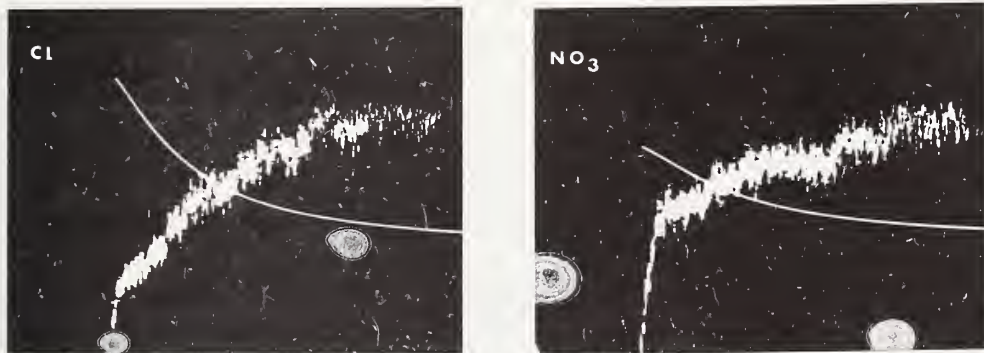
Fig. 4. Change in thickness, x, and repassivation ratio, R_p, after removal of the abrasion wheel of the tribo-ellipsometric apparatus for Ti 8-1-1 in 1N $NaNO_3$ at 25°C. The alloy is at +706 mV (SHE).

TITANIUM   ALLOY   (8-1-1)

in chloride (susceptible

and nitrate (non-susceptible)

Fig. 5.   A comparison of oscilloscope repassivation transients for
           Ti 8-1-1 in 1N NaCl and 1N NaNO$_3$ solutions at +706 mV (SHE)
           [Ellipsometric film growth - jagged trace; current - solid
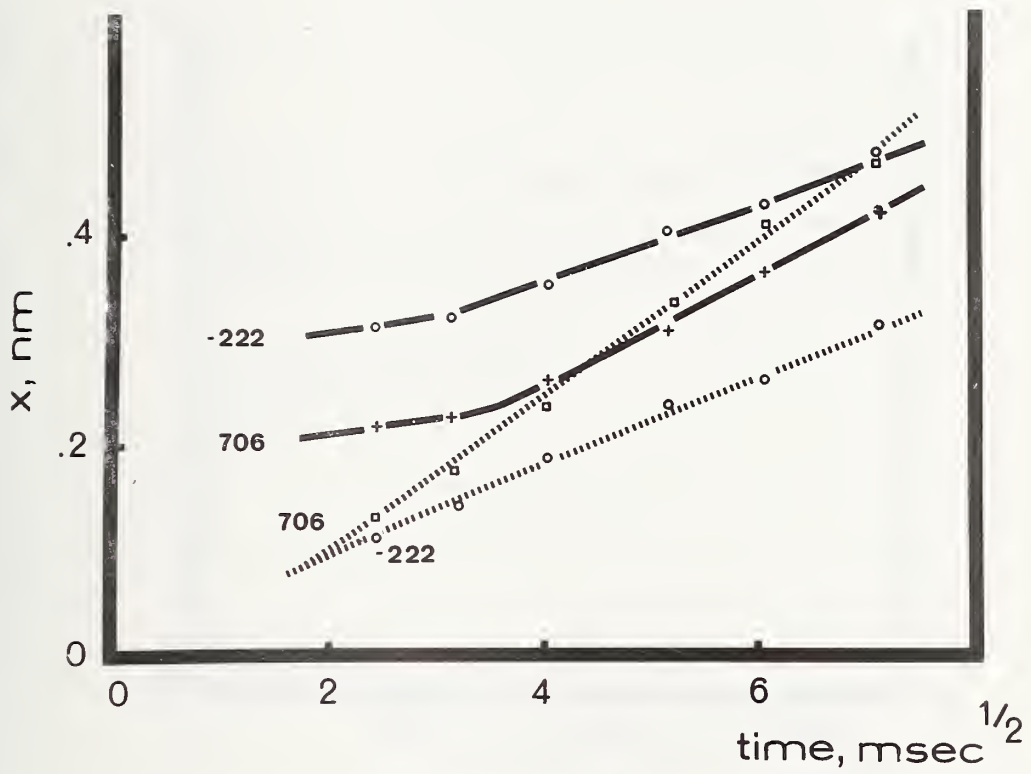   line trace].

Fig. 6.   Changes in film thickness, x, for Ti 8-1-1 in 1N NaNO₃
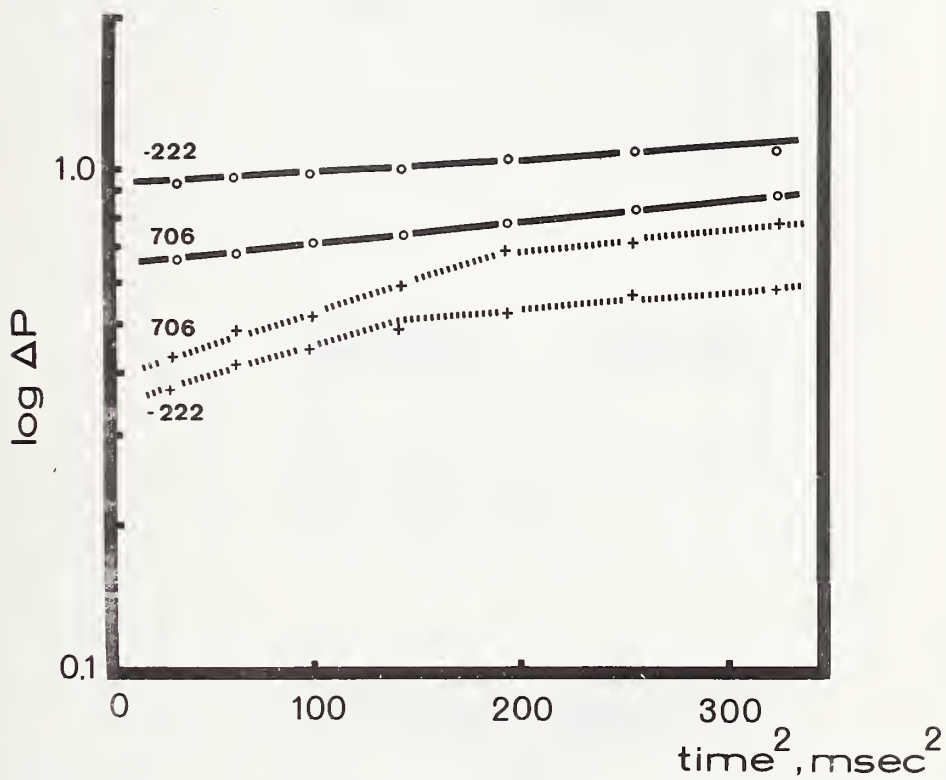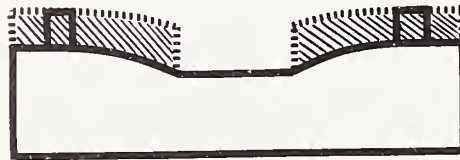   (— o — o) and 1N NaCl (......) at -222 and +706 mV (SHE)
         at 25°C.

Fig. 7. Changes in $\log_{10}\Delta P$ for Ti 8-1-1 in 1N $NaNO_3$ (— . — .) and 1N NaCl (.....) at -222 and +706 mV (SHE) at 25°C.
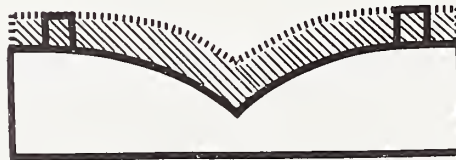
Fig. 8. Schematic of the effect of the Fleischmann-Thirsk model of
         oxide path nucleation and growth on substrate penetration by
         metal dissolution. (a) Nucleation of oxide patches at cessation
         of abrasion; (b) metal dissolution during lateral patch growth
         resulting in formation of localized crevices where patches
         coalesce (c).

70

DOCUMENT CONTROL DATA - R & D

Security classification of title, body of abstract and indexing annotation must be entered when the overall report is classified)

1 ORIGINATING ACTIVITY (Corporate author)	2a. REPORT SECURITY CLASSIFICATION
National Bureau of Standards Washington, D. C. 20234	Unclassified
	2b. GROUP

3 REPORT TITLE

The Role of Passive Film Growth Kinetics and Properties in Stress Corrosion and Crevice Corrosion Susceptibility

4. DESCRIPTIVE NOTES *(Type of report and inclusive dates)*
Technical Summary Report No. 4

5. AUTHOR(S) *(First name, middle initial, last name)*

J. Kruger
J. R. Ambrose

6. REPORT DATE	7a. TOTAL NO. OF PAGES	7b. NO. OF REFS

8a. CONTRACT OR GRANT NO.	9a. ORIGINATOR'S REPORT NUMBER(S)
NAONR 18-69, NR036-082	NBSIR 73-244
b. PROJECT NO. 3120448	
c.	9b. OTHER REPORT NO(S) *(Any other numbers that may be assigned this report)*
d.	

10. DISTRIBUTION STATEMENT

Distribution of this document is unlimited

11. SUPPLEMENTARY NOTES	12. SPONSORING MILITARY ACTIVITY
	Office of Naval Research

13 ABSTRACT

Repassivation kinetics of an AISI 304 stainless steel have been determined in 1.0N NaCl solutions using the triboellipsometry technique which permits measurement of film growth and total reaction rates following removal of the surface film by abrasion. Although deoxygenation of the solution resulted in little change in other film growth kinetics or the ratio of total change to film thickness (R_p), changing the solution pH affected both the mechanism and rate of film growth which resulted in increased rates of metal dissolution in acidic (pH3) and basic (pH11) solutions.

In neutral 1.0N NaCl solutions, where film growth increased with more positive applied potentials, the rate of metal dissolution during the repassivation transient was initially highest at the corrosion potential, but decreased with time as the surface became passivated.

The tribo-ellipsometry technique was used to determine repassivation kinetics and stress corrosion cracking (SCC) susceptibility for Ti-8Al-1Mo-1V alloy. Repassivation transient behavior in a 1.0N NaCl solution, where cracks have been found to propagate, was compared to that in a 1.0N NaNO3 solution where SCC susceptibility has never been detected.

Film growth kinetics in both solutions were consistent with a Fleischmann-Thirsk mechanism of oxide patch nucleation and two-dimensional growth, although the film growth rate was significantly slower in the 1.0N NaCl solution. This was in turn responsible for an increase in metal dissolution in a solution where crack propagation velocities have been measured, but at an apparent rate slower than necessary to propagate such cracks by metal dissolution alone.

14 KEY WORDS	LINK A		LINK B		LINK C	
	ROLE	WT	ROLE	WT	ROLE	WT
Stress corrosion cracking						
Repassivation kinetics						
Crevice corrosion						
Titanium alloys						
Stainless steel						
Ellipsometry						
Nitrates						
Chloride						
pH						
Dissolved oxygen						

The early stages of crevice corrosion of AISI 304 stainless steel in 1.0N NaCl solution have been detected using the ellipsometer to measure changes in optical properties occurring within the crevice between a polished metal surface and a glass plate. Changes in the ellipsometer parameters Δ and ψ begin almost immediately upon creation of the crevice and can be interpreted as resulting from a build-up of soluble species within the crevice solution, followed by an overall thinning of the protective film and general corrosion attack.

Such optical changes could not be reproduced by deoxygenation of the bulk solution without the presence of a crevice nor were they observed during experiments using a Ti-8Al-1Mo-1V alloy, which is not susceptible to crevice corrosion in the 1.0N NaCl at room temperature.

U.S. DEPT. OF COMM. BIBLIOGRAPHIC DATA SHEET	1. PUBLICATION OR REPORT NO. NBSIR-73-244	2. Gov't Accession No.	3. Recipient's Accession No.

4. TITLE AND SUBTITLE	5. Publication Date
The Role of Passive Film Growth Kinetics and Properties in Stress Corrosion and Crevice Corrosion Susceptibility	
	6. Performing Organization Code

7. AUTHOR(S) Jerome Kruger and John R. Ambrose	8. Performing Organization

9. PERFORMING ORGANIZATION NAME AND ADDRESS	10. Project/Task/Work Unit No. 3120448
NATIONAL BUREAU OF STANDARDS DEPARTMENT OF COMMERCE WASHINGTON, D.C. 20234	11. Contract/Grant No. NAONR 18-69, NR 036-082

12. Sponsoring Organization Name and Address	13. Type of Report & Period Covered Interim 3/1/72 - 2/28/73
Office of Naval Research Arlington, Virginia 22217	
	14. Sponsoring Agency Code

15. SUPPLEMENTARY NOTES

16. ABSTRACT (A 200-word or less factual summary of most significant information. If document includes a significant bibliography or literature survey, mention it here.)

Repassivation kinetics of an AISI 304 stainless steel have been determined in 1.0N NaCl solutions using the triboellipsometry technique which permits measurement of film growth and total reaction rates following removal of the surface film by abrasion. Although deoxygenation of the solution resulted in little change in either film growth kinetics or the ratio of total change to film thickness (R_p), changing the solution pH affected both the mechanism and rate of film growth which resulted in increased rates of metal dissolution in acidic (pH3) and basic (pH11) solutions.

The tribo-ellipsometry technique was also used to determine repassivation kinetics and stress corrosion cracking (SCC) susceptibility for Ti-8Al-1Mo-1V alloy. Repassivation transient behavior in a 1.0N NaCl solution, where cracks have been found to propagate, was compared to that in a 1.0N NaNO3 solution where SCC susceptibility has never been detected. Susceptibility was found to be related to film growth kinetics in the two solutions.

The early stages of crevice corrosion of AISI 304 stainless steel in 1.0N NaCl solution have been detected using the ellipsometer to measure changes in optical properties occurring within the crevice between a polished metal surface and a glass plate. Changes in the ellipsometer parameters Δ and ψ begin almost immediately upon creation of the crevice and can be interpreted as resulting from a build-up of soluble species within the crevice solution, followed by an overall thinning of the protective film and general corrosion attack.

17. KEY WORDS (Alphabetical order, separated by semicolons)
Chloride; Crevice corrosion; Dissolved oxygen; Ellipsometry; Nitrates; pH; Repassivation kinetics; Stainless steel; Stress corrosion cracking; Titanium alloys

18. AVAILABILITY STATEMENT	19. SECURITY CLASS (THIS REPORT)	21. NO. OF PAGES
XX UNLIMITED.	UNCLASSIFIED	
☐ FOR OFFICIAL DISTRIBUTION. DO NOT RELEASE TO NTIS.	20. SECURITY CLASS (THIS PAGE)	22. Price
	UNCLASSIFIED	